Table 4a
Number of 5′SAGE tags mapped to intronic region.

	NL	NT	T
Tag mapped to intron	1287	1253	1292
Total promoter region	952	981	1020
(tag number = 1)	788	813	863
(tag number ≧2)	164	168	157

ACOX2, *HGD*, *CYP3A5*, *KNG1* and *AGXT* were increased, while their 3′ transcripts (determined by 3′SAGE) were decreased in HCC. In contrast, both 5′ intronic transcripts and 3′ transcripts encoding *HFM1*, *SERPINA1*, *SUPT3H*, *A2M* and *TMEM176B* were similarly decreased in HCC. Taken together, these data imply that the canonical- and intronic-promoter activities of a subset of genes including *SAMD3*, *ACOX2*, *HGD*, *CYP3A5*, *KNG1* and *AGXT* might be differently regulated in HCC.

ACOX2 as a novel intronic gene deregulated in HCC

A subset of genes listed above may be transcribed from intronic regions specifically in HCC. Among these genes, we focused on the regulation of *ACOX2*, which is reported to be potentially involved in peroxisomal beta-oxidation and hepatocarcinogenesis [20]. The intron-origin expression of *ACOX2* increased six-fold in HCC compared with the NT by 5′SAGE, while the expression based on the 3′end was almost similar between HCC and NT lesions (Table 4b). Close examination of 5′SAGE data identified two potential intron-origin transcripts of *ACOX2* (Supplemental Fig. 4). The first (intronic-*ACOX2-1*) was initiated upstream of the tenth exon, whereas the second (intronic-*ACOX2-2*) was initiated upstream of the twelfth exon of *ACOX2* (Supplemental Fig. 4). The sequence of the intronic part was unique, and the remaining part of the sequence was shared with the canonical transcripts of *ACOX2*.

The expression of canonical *ACOX2* and the two types of intron-origin transcripts was investigated in NL, NT, and T tissues by RT-PCR (Fig. 1A). Although canonical *ACOX2* expression was decreased in T than in NL, the intron-origin transcript, particularly intronic-*ACOX2-1*, was increased in T. Intronic-*ACOX2-2* transcripts also showed a modest increase. We further evaluated the alteration of these transcripts in 19 HBV-HCCs, 20 HCV-HCCs, and 4 non-B, non-C HCCs, and their background liver tissues by canonical *ACOX2* and intronic-*ACOX2* specific real-time detection (RTD)-PCR. Although the expression of canonical *ACOX2* was decreased, the expression of intronic-*ACOX2* was significantly increased (Fig. 1B). Importantly, the gene expression ratios of intronic-to canonical *ACOX2* increased more in moderately differentiated HCCs (mHCC) than in well-differentiated HCCs (wHCC), suggesting the involvement of intronic-*ACOX2* expression on HCC progression.

Table 4b
Differentially expressed intronic promoter regions in HCC.

5′SAGE T/NL	3′SAGE T/NL	5′/3′ Ratio	Gene
Up-regulated			
9	1	9.00	Sterile alpha motif domain containing 3 (SAMD3)
6	0.89	6.74	Acyl-Coenzyme A oxidase 2, branched chain (ACOX2)
6	0.62	9.68	Homogentisate 1,2-dioxygenase (homogentisate oxidase) (HGD)
6	0.009	666.67	Cytochrome P450, family 3, subfamily A, polypeptide 5 (CYP3A5)
5	0.64	7.81	Kininogen 1 (KNG1)
4	0.36	11.11	Alanine-glyoxylate aminotransferase (AGXT)
4	1	4.00	Crystallin, alpha A (CRYAA)
Down-regulated			
0.13	1	0.13	HFM1, ATP-dependent DNA helicase homolog (*S. cerevisiae*) (HFM1)
0.25	0.51	0.49	Serpin peptidase inhibitor, clade A member 1 (SERPINA1)
0.25	1	0.25	Suppressor of Ty 3 Homolog (*S. cerevisiae*) (SUPT3H)
0.25	0.2	1.25	Alpha-2-macroglobulin (A2M)
0.25	0.083	3.13	Transmembrane protein 176B (TMEM176B)

3′SAGE, 3′-end serial analysis of gene expression; 5′SAGE, 5′-end serial analysis of gene expression; HCC, hepatocellular carcinoma; NL, normal liver; NT, non-tumor; T, tumor.

Discussion

This is the first comprehensive transcriptional analysis of tissue lesions of non-B, non-C HCC, background liver and NL using the 5′ SAGE method. Approximately 6.7% of our 5′SAGE tags showed no matching within the human genome, possibly due to the presence of a single nucleotide polymorphism (SNP) in the human genome. Out of the complete matched tags in the genome, 70% were assigned to unique positions and 30% to two or more loci. The tags with multiple matches with genomic loci were largely retrotransposon elements, repetitive sequences, and pseudogenes.

In this study, the analysis of non-B, non-C HCC enabled us to evaluate direct molecular changes associated with HCC without any bias of gene induction by virus infection. The gene expression profile based on our 5′SAGE tags revealed that *albumin (ALB)* and apolipoproteins were highly expressed in NL, indicating the massive production of plasma proteins in NL; these results are similar to those of our previous study using 3′SAGE [6]. Other genes such as *aldolase B (ALDOB)*, *antitrypsin (SERPINA1)*, and *haptoglobin (HP)* were also highly expressed in NL, in both the 5′SAGE and 3′SAGE libraries (Table 2) [6]. Comparison of the expression profiles among NL, background NT and T identified several differentially expressed transcripts in T. *Galectin-4 (LGALS4)* was up-regulated and *HAMP*, *NNMT*, *CYP2E1*, and *metallothionein* were down-regulated in HCC in accordance with previous findings (Table 3a) [8,9,21]. Moreover, *CLEC4G*, which was predominantly expressed in the sinusoidal endothelial cells of the liver, was down-regulated in HCC. In addition, we first found that *P antigen family, member 2 (PAGE2)* and *XAGE1A* were up-regulated in HCC (Table 3a, Supplemental Fig. 1). These genes were members of cancer-testis antigen that include MAGE-family genes. MAGE-family members were originally found to be up-regulated in HCV-related HCC, and reported to be useful as molecular markers and as possible target molecules for immunotherapy in human HCC [22]. In this study, we identified that these members of genes were also up-regulated in non B, non-C HCC. Thus, these genes may be useful as molecular markers and therapeutic targets for the treatment of a certain type of human HCC.

There existed some discrepancy between 5′SAGE and 3′SAGE results, even though they were derived from the same sample. Technical issues such as amplication error, difference of restriction enzyme, and annotation error have been described previously [14]. It is possible that 3′ transcripts might be more stable than 5′ transcripts by binding of ribosomal proteins during translation. Another possibility is the diversity of the transcriptional start and/or termination sites. One of the advantages of 5′SAGE analysis is the potential to determine the transcriptional start sites in each gene. Indeed, a recent study indicated the importance of an insulin splice variant in the pathogenesis of insulinomas [23]. Considering the diversity of 5′ends of genes, it is more appropriate to perform 5′SAGE in combination with 3′SAGE when determining the frequency of gene expression and identifying novel transcript variants.

Here, we were able to identify at least 12 intron-origin transcripts that were differentially expressed in HCC compared with the background liver or NL. These transcripts could not be identified by the 3′SAGE approach. We also performed detailed expression analysis of *ACOX2* that was involved in the beta-oxidation of peroxisome. We

Please cite this article as: Y. Hodo, et al., Comprehensive gene expression analysis of 5′-end of mRNA identified novel intronic transcripts associated with hepatocellular carcinoma, Genomics (2010), doi:10.1016/j.ygeno.2010.01.004

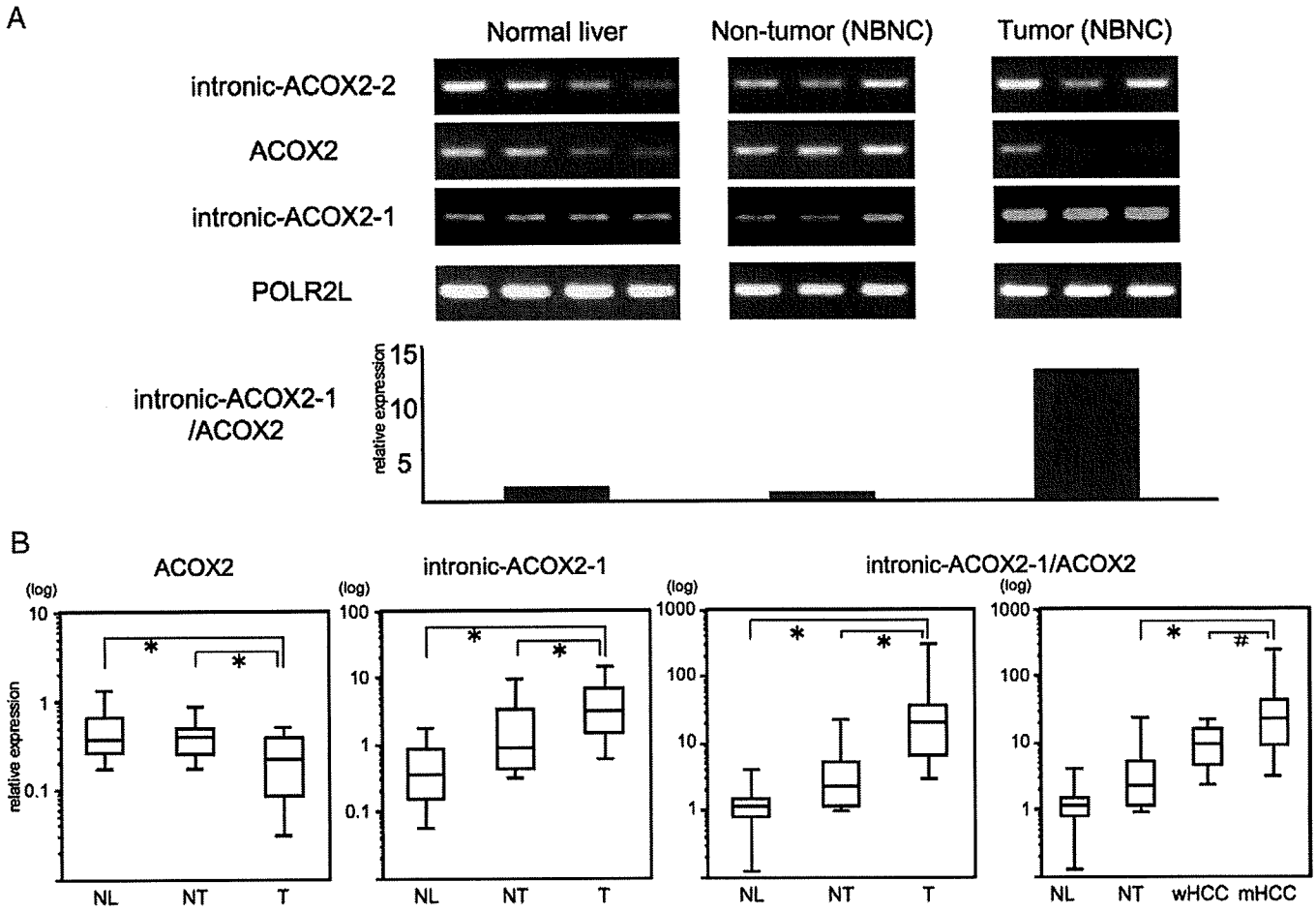

Fig. 1. (A) RT-PCR results of *ACOX2* and *ACOX2* intronic RNAs in independent NL, NT (non-B, non-C), and T (non-B, non-C) samples. RT-PCR was performed in triplicate for each sample-primer set from cDNA. The PCR products were semi-quantitatively analyzed with ImageJ software and calculated as levels relative to *polymerase (RNA) II (DNA directed) polypeptide L* (*POLR2L*). The bar graph indicates the expression ratio of intronic-ACOX2-1 to canonical ACOX2. The expression pattern of intron 1 was different from that of canonical *ACOX2*. (B) RTD-PCR analysis of *ACOX2* and *ACOX2* intronic RNAs in NL, T (HBV-related, HCV-related, and non-B, non-C), and NT tissues. Quantitative RTD-PCR was performed in duplicate for each sample-primer set from cDNA. Each sample was normalized relative to *POLR2L*. All HCC tissues were pathologically diagnosed as well differentiated HCC (wHCC) or moderately differentiated HCC (mHCC). Kruskal–Wallis tests and Mann–Whitney *U* tests were used for statistical analysis. ACOX2, acyl-Coenzyme A oxidase 2; HCC, hepatocellular carcinoma; NL, normal liver; NT, non-tumor; RT-PCR, reverse transcriptase-polymerase chain reaction; RTD-PCR, real-time detection-PCR; T, tumor. *$P<0.01$, #$P<0.05$.

were able to clone the intron-origin *ACOX2* RNAs (intronic-*ACOX2-1, 2*) for the first time and found that intronic-*ACOX2-1* was significantly overexpressed in T compared with NT and NL. The ratio of intronic-*ACOX2-1* and canonical *ACOX2* (relative intronic-*ACOX2*) was progressively up-regulated from NL via the background liver to HCC. Importantly, the expression of relative intronic-*ACOX2* was more up-regulated in moderately differentiated HCC than in well-differentiated HCC. The intronic difference in expression might be due to a polymorphism, since the 5′SAGE library for NL and T were from different people. The mechanisms of stepwise increase of intronic-*ACOX2* in the process of hepatocarinogenesis should be clarified in future.

ACOX2 is a rate-limiting enzyme of branched-chain acyl-CoA oxidase involved in the degradation of long branched fatty acid and bile acid intermediates in peroxisomes. *ACOX2* expression was associated with the differentiation state of hepatocytes and was repressed under the undifferentiated phase of human hepatoma cell lines [24]. A decreased *ACOX2* expression was also reported in prostate cancer [25]. Here, the expression of canonical *ACOX2* was decreased, while that of intronic-*ACOX2-1* was increased in HCC. The deduced amino acid of intronic-*ACOX2-1* encodes the C-terminal (from 386 to 681 amino acids) of canonical *ACOX2*, lacking the active sites for FAD binding and a fatty acid as the substrate, suggesting that the protein may be functionally departed [26]. The biological role of the increased intronic-*ACOX2-1* was not clear, but it might be reflected by the activation of peroxisome proliferators-activated receptor alpha (PPARA). It is reported that mice lacking ACOX1, another rate-limiting enzyme in peroxisomal straight-chain fatty acid oxidation, developed steatosis and HCC characterized by increased mRNA and protein expression of genes regulated by PPARα [27]. The importance of PPARα activation in HCC development has been recently reported using HCV core protein transgenic mice [28]. Moreover, the overexpression of alpha-methylacyl-CoA racemase (AMACR), an enzyme for branched-chain fatty acid beta-oxidation, is reported to be a reliable diagnostic marker of prostate cancer and is associated with the decreased expression of ACOX2 [25]. Therefore, the expression of intronic-*ACOX2-1* might open the door for further investigations of their potential clinical use, e.g., serving as diagnostic markers of HCC, although the functional relevance of this gene should be further clarified.

In conclusion, we report the first comprehensive transcriptional analysis of non-B, non-C HCC, NT background liver, and NL tissue, based on 5′SAGE. This study offers new insights into the transcriptional changes that occur during HCC development as well as the molecular mechanism of carcinogenesis in the liver. The results suggest the presence of unique intron-origin RNAs that are useful as diagnostic markers and may be used as new therapeutic targets.

Please cite this article as: Y. Hodo, et al., Comprehensive gene expression analysis of 5′-end of mRNA identified novel intronic transcripts associated with hepatocellular carcinoma, Genomics (2010), doi:10.1016/j.ygeno.2010.01.004

Material and methods

Samples

Samples were obtained from a 56-year-old man who had undergone surgical hepatic resection for the treatment of solitary HCC. Serological tests for hepatitis B surface (HBs) antigen and anti-HCV antibodies were negative. Tumor (T) and non-tumor (NT) tissue samples were separately obtained from the tumorous parts (diagnosed as moderately differentiated HCC) and non-tumorous parts (diagnosed as mild chronic hepatitis: F1A1) of the resected tissue. We also obtained five normal liver (NL) tissue samples from five patients who had undergone surgical hepatic resection because of metastatic liver cancer. None of the patients was seropositive for both HBs antigen and anti-HCV antibodies. Neither heavy alcohol consumption nor the intake of chemical agents was observed before surgical resection. All laboratory values related to hepatic function were within the normal range. All procedures and risks were explained verbally and provided in a written consent form.

We additionally used independent four NL tissue samples, 19 HBV-HCCs, 20 HCV-HCCs and 4 non-B, non-C HCCs, and their background liver tissue samples for reverse transcriptase-polymerase chain reaction (RT-PCR) and real-time detection (RTD)-PCR (Supplemental Table 1). Four non-B, non-C HCCs were histologically diagnosed as moderately differentiated HCCs, and the adjacent non-cancerous liver tissues were diagnosed as a normal liver, a chronic hepatitis, a pre-cirrhotic liver and a cryptogenic liver cirrhosis, respectively. None of the patients was seropositive for HBs antigen, anti-HBs antibodies, anti-hepatitis B core (HBc) antibodies and anti-HCV antibodies. Neither heavy alcohol consumption nor the intake of chemical agents was observed. Histological grading of the tumor was evaluated by two independent pathologists as described previously [16].

Generation of the 5′ SAGE library

5′SAGE libraries were generated as previously described [14]. Five to ten micrograms of poly(A)+RNA was treated with bacterial alkaline phosphatase (BAP; TaKaRa, Otsu, Japan). Poly(A)+RNA was extracted twice with phenol: chloroform (1:1), ethanol precipitated, and then treated with tobacco acid pyrophosphatase (TAP). Two to four micrograms of the BAP-TAP-treated poly(A)+RNA was divided into two aliquots and an RNA linker containing recognition sites for *Eco*RI/*Mme*I was ligated using RNA ligase (TaKaRa): one aliquot was ligated to a 5′-oligo 1 (5′-GGA UUU GCU GGU GCA GUA CAA CGA AUU CCG AC-3′) linker, and the other aliquot was ligated to a 5′-oligo 2 (5′-CUG CUC GAA UGC AAG CUU CUG AAU UCC GAC-3′) linker. After removing unligated 5′-oligo, cDNA was synthesized using RNaseH-free reverse-transcriptase (Superscript II, Invitrogen, Carlsbad, CA, USA) at 12 °C for 1 h and 42 °C for the next hour, using 10 pmol of dT adapter-primer (5′-GCG GCT GAA GAC GGC CTA TGT GGC CTT TTT TTT TTT TTT TTT-3′). After first-strand synthesis, RNA was degraded in 15 mM NaOH at 65 °C for 1 h. cDNA was amplified in a volume of 100 μl by PCR with 16 pmol of 5′ (5′ [biotin]-GGA TTT GCT GGT GCA GTA CAA-3′ or 5′[biotin]-CTG CTC GAA TGC AAG CTT CTG-3′) and 3′ (5′-GCG GCT GAA GAC GGC CTA TGT-3′) PCR primers. cDNA was amplified using 10 cycles at 94 °C for 1 min, 58 °C for 1 min, and 72 °C for 2 min. PCR products were digested with the *Mme*I type IIS restriction endonuclease (NEB, Pickering, Ontario, Canada). The digested 5′-terminal cDNA fragments were bound to streptavidin-coated magnetic beads (Dynal, Oslo, Norway). cDNA fragments that bound to the beads were directly ligated together in a reaction mixture containing T4 DNA ligase in a supplied buffer for 2.5 h at 16 °C. The ditags were amplified by PCR using the following primers: 5′ GGA TTT GCT GGT GCA GTA CA 3′ and 5′ CTG CTC GAA TGC AAG CTT CT 3′. The PCR products were analyzed by polyacrylamide gel electrophoresis (PAGE) and digested with *Eco*RI. The region of the gel containing the ditags was excised and the fragments were self-ligated to produce long concatamers that were then cloned into the *Eco*RI site of pZero 1.0 (Invitrogen). Colonies were screened by PCR using the M13 forward and reverse primers. PCR products containing inserts of more than 600 bp were sequenced with Big Dye terminator ver.3 and analyzed using a 3730 ABI automated DNA sequencer (Applied Biosystems, Foster City, CA, USA). All electrophoretograms were reanalyzed by visual inspection to check for ambiguous bases and to correct misreads. In this study, we obtained 19–20 bp tag information.

Association of the 5′SAGE tags with their corresponding genes

We attempted to align our 5′tags with the human genome (NCBI build 36, available from http://www.genome.ucsc.edu/) using the alignment program ALPS (http://www.alps.gi.k.u-tokyo.ac.jp/). Only tags that matched in sense orientation were considered in our analysis. The RefSeq database was searched for transcripts corresponding to the regions adjacent to the alignment location of each 5′tag.

RT-PCR

Total RNA was extracted using a ToTally RNA extraction kit (Ambion, Inc., Austin, TX, USA). Total RNA (500 ng) was reverse-transcribed in a 100-μl reaction solution containing 240 U of Moloney murine leukemia virus reverse transcriptase (Promega, Madison, WI, USA), 80 U of RNase inhibitor (Promega), 4.6 mM $MgCl_2$, 6.6 mM DTT, 1 mM dNTPs, and 2 mM random hexamer (Promega), at 42 °C for 1 h. PCR was performed in a 20-μl volume containing 0.5 U of AmpliTaq DNA polymerase (Applied Biosystems), 16.6 mM $(NH_4)_2SO_4$, 67 mM Tris–HCl, 6.7 mM $MgCl_2$, 10 mM 2-mercaptoethanol, 1 mM dNTPs, and 1.5 μM sense and antisense primers, using an ABI 9600 thermal cycler (Applied Biosystems). The amplification protocol included 28–30 cycles of 95 °C for 45 s, 58 °C for 1 min, and 72 °C for 1 min. Primer sequences are shown in Supplemental Table 2. RT-PCR was performed in triplicate for each sample-primer set. Each sample was normalized relative to *polymerase (RNA) II (DNA directed) polypeptide L (POLR2L)*. *POLR2L* is a housekeeping gene that showed relatively stable gene expression in various tissues [29]. The PCR products were semi-quantitatively analyzed with ImageJ software (http://rsb.info.nih.gov/ij/).

RTD-PCR

Intron-origin transcript expression was quantified using TaqMan Universal Master Mix (Applied Biosystems). The samples were amplified using an ABI PRISM 7900HT Sequence Detection System (Applied Biosystems). Using the standard curve methods, quantitative PCR was performed in duplicate for each sample-primer set. Each sample was normalized relative to *POLR2L*. The assay IDs used were Hs00185873_m1 for *ACOX2* and Hs00360764_m1 for *POLR2L*. The specific primers and probe sequence of intronic-*ACOX2-1* were 5′-TTCATAAAGTTGTGAGCA-GAGGAAA-3′ (forward), 5′-TGCACCACTTACTGAGCATCTACTC-3′ (reverse), and 5′-ACTTCTTACCTCAGAGCTG-3′ (probe).

Analysis of pathway network

MetaCore™ software (GeneGo Inc., St. Joseph, MI) was used to investigate the molecular pathway networks of non-B, non-C HCC, HBV-HCC and HCV-HCC. All genes up-regulated more than five-fold in all HCC libraries subjected to Enrichment analysis in GO process networks by default settings ($p<0.05$).

Statistical analysis

Kruskal–Wallis tests were used to compare the expression among normal liver, non-cancerous tissues, and HCC tissues. Mann–Whitney *U* tests were also used to evaluate the statistical significance of ACOX2

Please cite this article as: Y. Hodo, et al., Comprehensive gene expression analysis of 5′-end of mRNA identified novel intronic transcripts associated with hepatocellular carcinoma, Genomics (2010), doi:10.1016/j.ygeno.2010.01.004

gene expression levels between two groups. All statistical analyses were performed using R (http://www.r-project.org/).

Acknowledgments

The authors would like to thank Mr. Shungo Deshimaru and Ms. Keiko Harukawa for technical assistance.

Appendix A. Supplementary data

Supplementary data associated with this article can be found, in the online version, at doi:10.1016/j.ygeno.2010.01.004.

References

[1] H.B. El-Serag, K.L. Rudolph, Hepatocellular carcinoma: epidemiology and molecular carcinogenesis, Gastroenterology 132 (2007) 2557–2576.
[2] Y. Yokoi, S. Suzuki, S. Baba, K. Inaba, H. Konno, S. Nakamura, Clinicopathological features of hepatocellular carcinomas (HCCs) arising in patients without chronic viral infection or alcohol abuse: a retrospective study of patients undergoing hepatic resection, J. Gastroenterol. 40 (2005) 274–282.
[3] R.N. Aravalli, C.J. Steer, E.N. Cressman, Molecular mechanisms of hepatocellular carcinoma, Hepatology 48 (2008) 2047–2063.
[4] D.J. Duggan, M. Bittner, Y. Chen, P. Meltzer, J.M. Trent, Expression profiling using cDNA microarrays, Nat. Genet. 21 (1999) 10–14.
[5] V.E. Velculescu, L. Zhang, B. Vogelstein, K.W. Kinzler, Serial analysis of gene expression, Science 270 (1995) 484–487.
[6] T. Yamashita, S. Hashimoto, S. Kaneko, S. Nagai, N. Toyoda, T. Suzuki, K. Kobayashi, K. Matsushima, Comprehensive gene expression profile of a normal human liver, Biochem. Biophys. Res. Commun. 269 (2000) 110–116.
[7] S. Hashimoto, S. Nagai, J. Sese, T. Suzuki, A. Obata, T. Sato, N. Toyoda, H.Y. Dong, M. Kurachi, T. Nagahata, K. Shizuno, S. Morishita, K. Matsushima, Gene expression profile in human leukocytes, Blood 101 (2003) 3509–3513.
[8] H. Okabe, S. Satoh, T. Kato, O. Kitahara, R. Yanagawa, Y. Yamaoka, T. Tsunoda, Y. Furukawa, Y. Nakamura, Genome-wide analysis of gene expression in human hepatocellular carcinomas using cDNA microarray: identification of genes involved in viral carcinogenesis and tumor progression, Cancer. Res. 61 (2001) 2129–2137.
[9] Y. Shirota, S. Kaneko, M. Honda, H.F. Kawai, K. Kobayashi, Identification of differentially expressed genes in hepatocellular carcinoma with cDNA microarrays, Hepatology 33 (2001) 832–840.
[10] T. Yamashita, M. Honda, S. Kaneko, Application of serial analysis of gene expression in cancer research, Curr. Pharm. Biotechnol. 9 (2008) 375–382.
[11] Y. Suzuki, H. Taira, T. Tsunoda, J. Mizushima-Sugano, J. Sese, H. Hata, T. Ota, T. Isogai, T. Tanaka, S. Morishita, K. Okubo, Y. Sakaki, Y. Nakamura, A. Suyama, S. Sugano, Diverse transcriptional initiation revealed by fine, large-scale mapping of mRNA start sites, EMBO Rep. 2 (2001) 388–393.
[12] K. Kimura, A. Wakamatsu, Y. Suzuki, T. Ota, T. Nishikawa, R. Yamashita, J. Yamamoto, M. Sekine, K. Tsuritani, H. Wakaguri, S. Ishii, T. Sugiyama, K. Saito, Y. Isono, R. Irie, N. Kushida, T. Yoneyama, R. Otsuka, K. Kanda, T. Yokoi, H. Kondo, M. Wagatsuma, K. Murakawa, S. Ishida, T. Ishibashi, A. Takahashi-Fujii, T. Tanase, K. Nagai, H. Kikuchi, K. Nakai, T. Isogai, S. Sugano, Diversification of transcriptional modulation: large-scale identification and characterization of putative alternative promoters of human genes, Genome. Res. 16 (2006) 55–65.
[13] T. Shiraki, S. Kondo, S. Katayama, K. Waki, T. Kasukawa, H. Kawaji, R. Kodzius, A. Watahiki, M. Nakamura, T. Arakawa, S. Fukuda, D. Sasaki, A. Podhajska, M. Harbers, J. Kawai, P. Carninci, Y. Hayashizaki, Cap analysis gene expression for high-throughput analysis of transcriptional starting point and identification of promoter usage, Proc. Natl. Acad. Sci. U. S. A. 100 (2003) 15776–15781.
[14] S. Hashimoto, Y. Suzuki, Y. Kasai, K. Morohoshi, T. Yamada, J. Sese, S. Morishita, S. Sugano, K. Matsushima, 5′-end SAGE for the analysis of transcriptional start sites, Nat. Biotechnol. 22 (2004) 1146–1149.
[15] T. Yamashita, S. Kaneko, S. Hashimoto, T. Sato, S. Nagai, N. Toyoda, T. Suzuki, K. Kobayashi, K. Matsushima, Serial analysis of gene expression in chronic hepatitis C and hepatocellular carcinoma, Biochem. Biophys. Res. Commun. 282 (2001) 647–654.
[16] T. Yamashita, M. Honda, H. Takatori, R. Nishino, H. Minato, H. Takamura, T. Ohta, S. Kaneko, Activation of lipogenic pathway correlates with cell proliferation and poor prognosis in hepatocellular carcinoma, J. Hepatol. 50 (2009) 100–110.
[17] J.S. Mattick, Introns: evolution and function, Curr. Opin. Genet. Dev. 4 (1994) 823–831.
[18] J.S. Mattick, I.V. Makunin, Non-coding RNA, Hum. Mol. Genet. 15 (Spec No 1) (2006) R17–29.
[19] R. Louro, A.S. Smirnova, S. Verjovski-Almeida, Long intronic noncoding RNA transcription: expression noise or expression choice? Genomics 93 (2009) 291–298.
[20] S. Yu, S. Rao, J.K. Reddy, Peroxisome proliferator-activated receptors, fatty acid oxidation, steatohepatitis and hepatocarcinogenesis, Curr. Mol. Med. 3 (2003) 561–572.
[21] N. Kondoh, T. Wakatsuki, A. Ryo, A. Hada, T. Aihara, S. Horiuchi, N. Goseki, O. Matsubara, K. Takenaka, M. Shichita, K. Tanaka, M. Shuda, M. Yamamoto, Identification and characterization of genes associated with human hepatocellular carcinogenesis, Cancer. Res. 59 (1999) 4990–4996.
[22] Y. Kobayashi, T. Higashi, K. Nouso, H. Nakatsukasa, M. Ishizaki, T. Kaneyoshi, N. Toshikuni, K. Kariyama, E. Nakayama, T. Tsuji, Expression of MAGE, GAGE and BAGE genes in human liver diseases: utility as molecular markers for hepatocellular carcinoma, J. Hepatol. 32 (2000) 612–617.
[23] A.H. Minn, M. Kayton, D. Lorang, S.C. Hoffmann, D.M. Harlan, S.K. Libutti, A. Shalev, Insulinomas and expression of an insulin splice variant, Lancet 363 (2004) 363–367.
[24] H. Stier, H.D. Fahimi, P.P. Van Veldhoven, G.P. Mannaerts, A. Volkl, E. Baumgart, Maturation of peroxisomes in differentiating human hepatoblastoma cells (HepG2): possible involvement of the peroxisome proliferator-activated receptor alpha (PPAR alpha), Differentiation 64 (1998) 55–66.
[25] S. Zha, S. Ferdinandusse, J.L. Hicks, S. Denis, T.A. Dunn, R.J. Wanders, J. Luo, A.M. De Marzo, W.B. Isaacs, Peroxisomal branched chain fatty acid beta-oxidation pathway is upregulated in prostate cancer, Prostate 63 (2005) 316–323.
[26] K. Tokuoka, Y. Nakajima, K. Hirotsu, I. Miyahara, Y. Nishina, K. Shiga, H. Tamaoki, C. Setoyama, H. Tojo, R. Miura, Three-dimensional structure of rat-liver acyl-CoA oxidase in complex with a fatty acid: insights into substrate-recognition and reactivity toward molecular oxygen, J. Biochem. 139 (2006) 789–795.
[27] K. Meyer, Y. Jia, W.Q. Cao, P. Kashireddy, M.S. Rao, Expression of peroxisome proliferator-activated receptor alpha, and PPARalpha regulated genes in spontaneously developed hepatocellular carcinomas in fatty acyl-CoA oxidase null mice, Int. J. Oncol. 21 (2002) 1175–1180.
[28] N. Tanaka, K. Moriya, K. Kiyosawa, K. Koike, F.J. Gonzalez, T. Aoyama, PPARalpha activation is essential for HCV core protein-induced hepatic steatosis and hepatocellular carcinoma in mice, J. Clin. Invest. 118 (2008) 683–694.
[29] C. Rubie, K. Kempf, J. Hans, T. Su, B. Tilton, T. Georg, B. Brittner, B. Ludwig, M. Schilling, Housekeeping gene variability in normal and cancerous colorectal, pancreatic, esophageal, gastric and hepatic tissues, Mol. Cell. Probes. 19 (2005) 101–109.

Please cite this article as: Y. Hodo, et al., Comprehensive gene expression analysis of 5′-end of mRNA identified novel intronic transcripts associated with hepatocellular carcinoma, Genomics (2010), doi:10.1016/j.ygeno.2010.01.004

Circulation
Cardiovascular Genetics
JOURNAL OF THE AMERICAN HEART ASSOCIATION
American Heart Association
Learn and Live

Altered Hepatic Gene Expression Profiles Associated With Myocardial Ischemia

Hiroshi Ootsuji, Masao Honda, Shuichi Kaneko, Soichiro Usui, Masaki Okajima, Hikari Okada, Yoshio Sakai, Toshinari Takamura, Katsuhisa Horimoto and Masayuki Takamura

Circ Cardiovasc Genet 2010;3;68-77; originally published online Dec 1, 2009;
DOI: 10.1161/CIRCGENETICS.108.795484
Circulation: Cardiovascular Genetics is published by the American Heart Association. 7272 Greenville Avenue, Dallas, TX 72514
 Print ISSN: 1942-325X. Online ISSN: 1942-3268

Altered Hepatic Gene Expression Profiles Associated With Myocardial Ischemia

Hiroshi Ootsuji, MD; Masao Honda, MD, PhD; Shuichi Kaneko, MD, PhD; Soichiro Usui, MD, PhD; Masaki Okajima, MD, PhD; Hikari Okada, MS; Yoshio Sakai, MD, PhD; Toshinari Takamura, MD, PhD; Katsuhisa Horimoto, PhD; Masayuki Takamura, MD, PhD

Background—Acute coronary syndrome is sometimes accompanied by accelerated coagulability, lipid metabolism, and inflammatory responses, which are not attributable to the cardiac events alone. We hypothesized that the liver plays a pivotal role in the pathophysiology of acute coronary syndrome. We simultaneously analyzed the gene expression profiles of the liver and heart during acute myocardial ischemia in mice.

Methods and Results—Mice were divided into 3 treatment groups: sham operation, ischemia/reperfusion, and myocardial infarction. Mice with liver ischemia/reperfusion were included as additional controls. Marked changes in hepatic gene expression were observed after 24 hours, despite the lack of histological changes in the liver. Genes related to tissue remodeling, adhesion molecules, and morphogenesis were significantly upregulated in the livers of mice with myocardial ischemia/reperfusion or infarction but not in those with liver ischemia/reperfusion. Myocardial ischemia, but not changes in the hemodynamic state, was postulated to significantly alter hepatic gene expression. Moreover, detailed analysis of the signaling pathway suggested the presence of humoral factors that intervened between the heart and liver. To address these points, we used isolated primary hepatocytes and showed that osteopontin released from the heart actually altered the signaling pathways of primary hepatocytes to those observed in the livers of mice under myocardial ischemia. Moreover, osteopontin stimulated primary hepatocytes to secrete vascular endothelial growth factor-A, which is important for tissue remodeling.

Conclusions—Hepatic gene expression is potentially regulated by cardiac humoral factors under myocardial ischemia. These results provide new insights into the pathophysiology of acute coronary syndrome. (***Circ Cardiovasc Genet.* 2010;3:68-77.**)

Key Words: coronary disease ■ genetics ■ liver ■ myocardial infarction

In addition to chest pain, acute coronary syndrome (ACS) is sometimes accompanied by systemic manifestations, such as proinflammatory responses, activation of the coagulation-fibrinolytic system, and lipid metabolism.[1–3] These are considered to be systemic reactions involving multiple organs, which exacerbate the cardiac events.

Clinical Perspective on p 77

C-reactive protein, coagulation factors, and protein C, the levels of which fluctuate in ACS, are liver-specific factors. Although these reports were based on a limited number of factors, the observations suggest a close relation between the liver and myocardial ischemia and imply that the liver plays a pivotal role in the pathophysiology of ACS.

cDNA microarray technology allows simultaneous analysis of the expression levels of thousands of genes. Genome-based expression profiling provides useful information on the molecular pathogenesis of various diseases as well as disease progression and prognosis.[4–7] Previous microarray studies have examined the molecular dynamics of the myocardium induced by myocardial ischemia.[8,9] However, global gene expression analyses applied to the liver affected by myocardial ischemia have not been reported.

In this study, we examined the responses of hepatic gene expression to myocardial ischemia. Given the systemic inflammation that characterizes ACSs, we postulated that regulation of hepatic genes occurs by inflammatory mediators and not by alterations in hemodynamics or hepatic perfusion. Therefore, we used whole-genome transcriptional profiling to identify hepatic genes selectively regulated in myocardial ischemia.

Methods

This study was approved by institutional and governmental animal research committees and was conducted in accordance with the *Guide for the Care and Use of Laboratory Animals* published by the US National Institutes of Health (NIH publication No. 85-23, revised 1996). C57BL/6J mice (n=46; body weight, 24.1±1.4 g; 8 to 10

Received June 1, 2008; accepted November 10, 2009.

From the Department of Disease Control and Homeostasis (H. Ootsuji, M.H., S.K., S.U., M.O., H. Okada, Y.S., T.T., M.T.), Kanazawa University Graduate School of Medical Science, Kanazawa University, Kanazawa, Japan; and National Institute of Advanced Industrial Science and Technology (K.H.), Tokyo, Japan.

The online-only Data Supplement is available at http://circgenetics.ahajournals.org/cgi/content/full/CIRCGENETICS.108.795484.

Correspondence to Shuichi Kaneko, MD, PhD, Department of Disease Control and Homeostasis, Kanazawa University Graduate School of Medical Science, Kanazawa University, 13-1 Takara-machi, Kanazawa 920-8641, Japan. E-mail skaneko@m-kanazawa.jp

Circ Cardiovasc Genet **is available at http://circgenetics.ahajournals.org** **DOI: 10.1161/CIRCGENETICS.108.795484**

Table 1. Biochemical Assessment

		6 h				24 h			
	Before Operation	Sham	I/R	Infarction	Liver I/R	Sham	I/R	Infarction	Liver I/R
No.	5	5	5	5	5	6	5	5	5
CPK, U/L	944±98	5031±646	11597±1272*	19830±1154*	8673±1379	1702±181	1913±184	2939±515†	1595±349
AST, U/L	94±4	674±41	899±21*	1858±59*	414±43	200±19	277±14	661±28*	163±22
ALT, U/L	58±4	119±9	115±6	153±7	143±18	46±3	64±6	107±11*	42±3
LDH, U/L	652±32	2684±206	3432±80†	5264±111*	2478±446	681±72	867±37	2095±164*	862±209

Values are presented as mean±SE. CPK indicates creatine kinase; AST, aspartate aminotransferase; ALT, alanine aminotransferase; and LDH, lactate dehydrogenase.

*$P<0.01$ compared with sham.

†$P<0.05$ compared with sham.

weeks of age; Charles River Laboratories, Yokohama, Japan) were divided into the following treatment groups: sham operation (n=11), ischemia/reperfusion (I/R; n=10), myocardial infarction (MI; n=10), liver I/R (n=10), and sham operation plus hydralazine (n=5). Hepatic gene expression was evaluated among these groups, and the results were further investigated in primary mouse hepatocytes.

Additional Methods

An expanded Methods section containing details of animal surgery, hydralazine group, liver I/R group, blood sampling and analysis, histopathological analysis, blood pressure and heart rate measurements, microarray experiments, processing of cDNA microarray data, extraction of significantly upregulated cardiac and hepatic genes, pathway analysis, ELISA for secreted osteopontin and vascular endothelial growth factor (*VEGF*), primary hepatocyte experiments, and quantitative real-time detection polymerase chain reaction (RTD-PCR) is available in the online-only Data Supplement.

All microarray data have been deposited in the National Center for Biotechnology Information Gene Expression Omnibus database with the series accession number GSE14843.

Data Analysis

The data are presented as the mean±SEM for each group of mice and were analyzed by ANOVA with Bonferroni post hoc test for multiple comparisons. Statistical analyses of blood sampling, blood pressure, and heart rate were performed with the Steel (heterogeneity of variance) multicomparison test. Significance was set at $P<0.05$. Statistical analyses were performed with SAS statistical software (SAS Institute Japan, Tokyo, Japan).

Results

Establishment of Cardiac I/R or MI in Mice

Cardiac I/R or MI was successfully induced in normal C57BL/6J mice. The levels of cardiac enzymes, such as creatine kinase, aspartate aminotransferase, and lactate dehydrogenase, increased significantly after 6 hours in the I/R group and showed markedly greater increases in the infarction group compared with the sham group (Table 1). In addition, the normalization of these enzyme levels was reduced after 24 hours in the infarction group.

Histologically, azan or hematoxylin/eosin staining showed wall thinning, coagulation necrosis, and transmural fibrosis in the risk area in the infarction group but not in the I/R group (data not shown). As shown in Table 2, no significant differences were found in heart rate or blood pressure after 24 hours compared with the preoperative values in the sham and I/R groups, whereas a decrease in blood pressure was found in the infarction group.

Histological Assessment of the Liver After Cardiac I/R or MI

The I/R and infarction groups showed a minimal, but transient, increase in alanine aminotransferase ALT. Although alanine aminotransferase may be released from the myocardium[10] rather than from the liver, to exclude the effect of the transient change in hepatic venous pressure associated with cardiogenic shock, we examined histological changes in the liver after myocardial I/R or infarction. No histological abnormalities were observed in the shocked liver, as indicated by the lack of hepatocyte necrosis in acinar zone 3 in the sham, I/R, and infarction groups (Figure 1a, 1c, 1e, and 1g; hematoxylin/eosin staining). In addition, no signs of liver congestion were observed, as indicated by the lack of dilatation of the terminal hepatic venules and adjacent sinusoids in the sham, I/R, or infarction group (Figure 1b, 1d, 1f, and 1h; silver staining).

On transmission electron microscopy, no ischemic changes, such as swelling or loss of cristae in the mitochondria, a mixed irregular pattern or swelling of the rough endoplasmic reticulum, or dilatation or indistinct appearance of the sinusoids, were observed in the sham, I/R, or infarction group (Figure 2A through 2C). Based on these results, histological analysis did not demonstrate the presence of shock or congestive liver in the I/R or infarction group.

Changes in the Hepatic Gene Expression Profile After Cardiac I/R or MI

Although no histological changes were observed in the liver after cardiac I/R or MI, significant changes in gene expression were noted. Hierarchical clustering analysis, which is a nonsupervised learning method that includes 23 281 nonfil-

Table 2. HR, sBP, and mBP

		24 h		
	Before Operation	Sham	I/R	Infarction
HR, bpm	575±27	553±30	553±27	568±16
sBP, mm Hg	105±2	102±2	95±1	80±4*
mBP, mm Hg	78±3	74±2	63±2	56±4†

Values are presented as mean±SE. HR indicates heart rate; sBP, systolic blood pressure; and mBP, mean blood pressure.

*$P<0.01$ compared with sham.

†$P<0.05$ compared with sham.

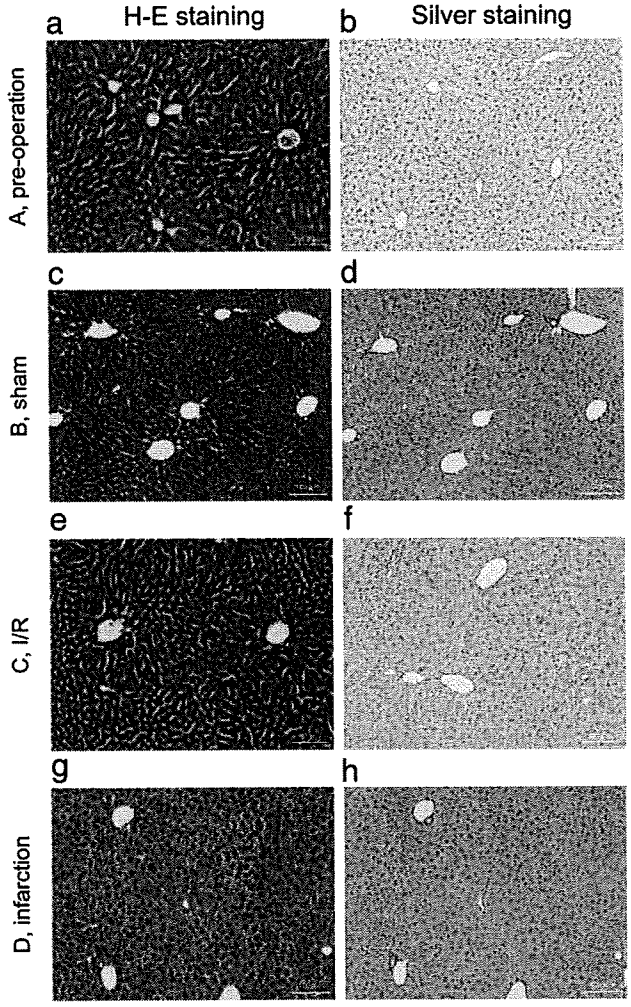

Figure 1. Histological comparison of hematoxylin/eosin staining and silver staining of the liver after 24 hours. Preoperation (A), sham (B), I/R (C), and infarction (D). Scale bars represent 100 μm. Hematoxylin/eosin staining (a, c, e, and g); silver staining (b, d, f, and h). No indication of shock or congestive liver was observed in any group (magnification, ×200).

tered genes, produced clusters for the I/R or infarction group and the sham-operated group (data not shown). Because nonfiltered genes may include those that are unchanged in all samples, which generated "noise" that prevented efficient gene clustering, we filtered out these genes with different stringency and performed hierarchical clustering. Hierarchical clustering with 9165 (log-ratio variations >40th percentile) or 5156 (log-ratio variations >50th percentile) filtered genes clearly demonstrated clusters for the I/R or infarction group after 24 hours, for the I/R or infarction group after 6 hours, and for the sham group after 6 and 24 hours (supplemental Figure I). Hierarchical clustering with 773 (log-ratio variations >80th percentile) or 96 (log-ratio variations >90th percentile) filtered genes showed more detailed and clearer clusters for the I/R group after 24 hours, for the infarction group after 24 hours, for the I/R or infarction group after 6 hours, and for the sham group after 6 and 24 hours (Figure 3). Thus, by filtering out "noise" genes, more detailed and clearer clustering could be obtained, thus addressing the reliability of the analysis.[11] The increased robustness (R-

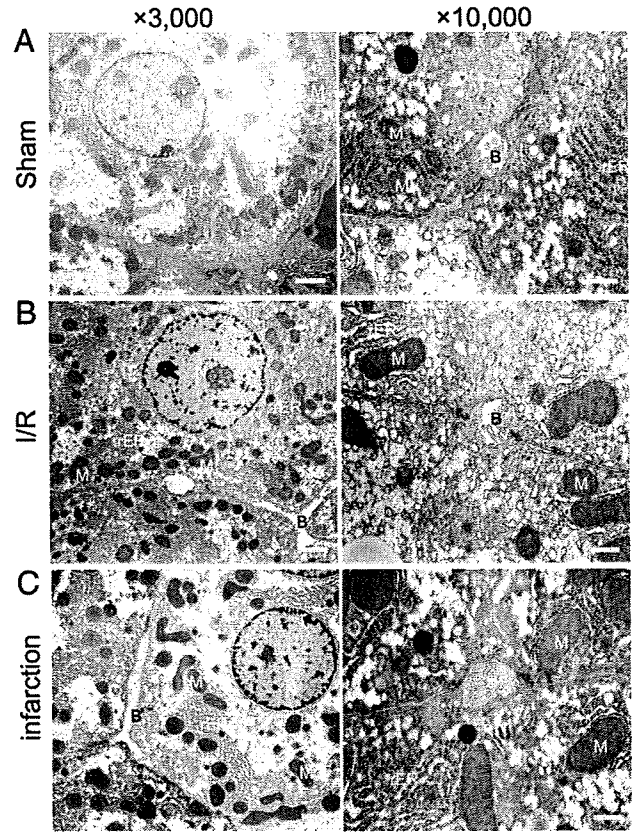

Figure 2. Representative electron microphotographs of the liver after 24 hours. Sham (A), I/R (B), and infarction (C). Scale bars represent 2 μm on the left (magnification, ×3000) and 500 nm on the right (magnification, ×10 000). No indication of shocked liver was observed in any group. M indicates mitochondria; rER, rough endoplasmic reticulum; B, bile canaliculi; N, nucleus.

index) and decreased discrepancy (D-index) of clustering with filtering conditions supported this finding (supplemental Figure I; expanded Methods and Results).

Class prediction analysis, a supervised learning method based on the compound covariate predictor, was performed with various clinical parameters, including provocation (I/R or infarction), 6 hours (I/R or infarction after 6 hours), 24 hours (I/R or infarction after 24 hours), and time (sham or 6 hours, sham or 24 hours, and 6 or 24 hours). The results

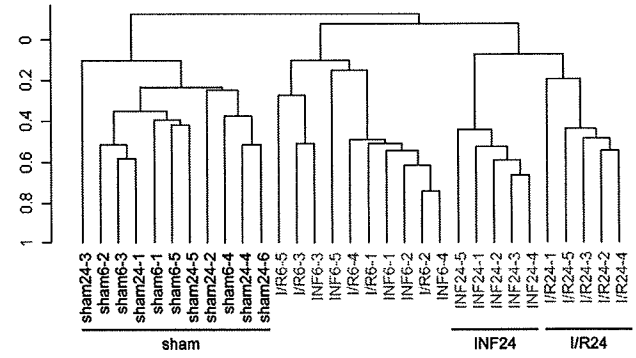

Figure 3. Hierarchical clustering analysis with 96 filtered genes (genes with log-ratio variation in the 90th percentile and data missing >5% were excluded). The resulting dendrogram shows clear clusters for the I/R group after 24 hours, the infarction group after 24 hours, and the sham group after 6 and 24 hours.

Table 3. Class Prediction Analysis (Supervised Learning Methods)

Classifier Category	Clinical Group	Total No. of Classes	No. of Cases Misclassified	Classifier *P*	Mean Percent of Correct Classification	No. of Genes in the Classifiers ($P<0.002$)
Provocation	I/R	10	2	0.02	80	85
	INF	10	2			
6 h	I/R	5	2	0.48	50	23
	INF	5	3			
24 h	I/R	5	0	0.015	100	218
	INF	5	0			
Time	Sham	11	0	0.001	90	644
	6 h	10	2			
	Sham	11	0	<0.0005	95	3380
	24 h	10	1			
	6 h	10	1	0.004	85	747
	24 h	10	2			

INF indicates infarction.

indicated that provocation, 24 hours, and time significantly classified these models (Table 3).

Both nonsupervised and supervised learning methods indicated differences in hepatic gene expression profiling among sham, 6 hours, and 24 hours after heart provocation, and different heart provocation (I/R or infarction) may generate differences in hepatic gene expression, especially 24 hours after provocation.

Identification of Genes Differentially Expressed Between I/R and Infarction

Because the filtering process may result in loss of important genes, for identification of differentially expressed genes among different groups, we used a class comparison analysis tool (http://linus.nci.nih.gov/BRB-ArrayTools.html). Class comparison analysis ($P<0.0005$) among the 5 groups (ie, sham, I/R-6, I/R-24, infarction-6, and infarction-24) was performed, and genes that were differentially expressed among the 5 groups were extracted. On 1-way hierarchical clustering analysis of the extracted genes and heat map, 6 gene clusters were assigned on the basis of the gene expression patterns (Figure 4). Of the 6 groups, group 2 showed significant upregulation for I/R and infarction after 24 hours compared with the other groups. Group 3 showed upregulation for I/R, but not for infarction, after 24 hours. Group 4 showed downregulation for I/R and infarction after 24 hours compared with the other groups. Group 5 showed downregulation for infarction after 24 hours compared with the other groups. Representative genes (>3-fold difference in *t* value) and frequent pathways observed in each group (based on the MetaCore database) are listed in supplemental Tables I through IV.

Interestingly, in group 2, genes related to tissue remodeling, adhesion molecules, and morphogenesis were significantly upregulated. This may be related to the induction of tissue repair factors, such as antigenic factor and myocardiogenic factors, associated with I/R or infarction. In addition, genes involved in the cell cycle and apoptosis and neuron-related genes, such as retinoblastoma 1, angiopoietin-like 4, apoptotic peptidase-activating factor 1, transformation-related protein 53 (*p53*), and Eph receptor B1, were preferentially expressed. The expression of group 2 genes was significantly correlated with serum creatine kinase levels, suggesting that these genes reflect the severity of cardiac damage. Especially, ($R=0.856$, $P<e^{-07}$) and apoptotic peptidase-activating factor 1 ($R=0.856$, $P<e^{-07}$) were highly correlated with creatine kinase (supplemental Table I).

In group 3, in addition to the genes described earlier, chemokine and hormone gene pathways involved in interleukin (IL)-8 and androgen or estrogen receptor signaling were upregulated, suggesting that more tissue repair and bioreactive signaling pathways were activated. This may reflect the presence of a living myocyte I/R condition. In group 4, genes involved in lipid catabolism, immune response, proteolysis, and oxidative stress, such as apolipoprotein A-II, CD7 antigen, and reduced nicotinamide-adenine dinucleotide phosphate oxidase 1, were downregulated in the infarction and I/R groups after 24 hours. In group 5, genes involved in muscle and neurite morphogenesis, such as myosin (heavy polypeptide 11, smooth muscle) and ephrin A5, were significantly downregulated in the infarction group after 24 hours.

Effects of Hemodynamic State on Hepatic Gene Expression Profile

To exclude the possibility that changes in hemodynamic state induced alterations in hepatic gene expression, we examined the livers of mice subjected to liver I/R. For liver I/R, gentle occlusion of the hepatic artery and portal vein was applied so that the extent of liver injury was comparable with those in the myocardial I/R and infarction models (Table 1).

We analyzed the gene expression profile of the liver I/R group by using the same extracted genes as shown in Figure 4. The gene expression patterns induced in the myocardial I/R and infarction groups are clearly different from those in the liver I/R group (Figure 5), except for the group 3 gene cluster in myocardial I/R. It should be noted that the group 3 gene cluster was upregulated in the myocardial I/R group at 24

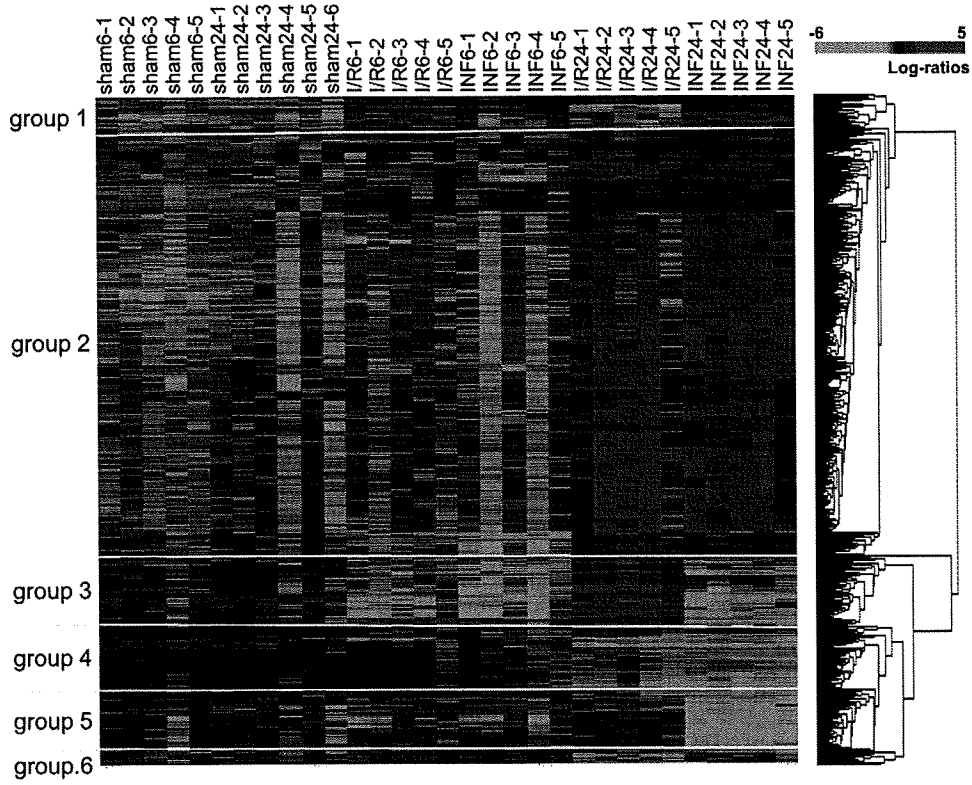

Figure 4. One-way hierarchical clustering and a heat map of 1166 genes that were extracted by class comparison analysis ($P<0.0005$). Each column corresponds to a sample, and each row represents a gene. The gene cluster data are graphically presented as colored images: red indicates upregulated genes, and green indicates downregulated genes. The genes with the most similar patterns of expression are adjacent to one another. Detailed definitions of each group are given in the text. Representative genes and frequently observed pathways are listed in supplemental Tables I through IV.

hours after provocation, whereas it was upregulated from 6 hours after provocation in the liver I/R group. Therefore, the delayed changes in hepatic gene expression in the myocardial I/R and infarction models may be due to different mechanisms resulting from liver I/R.

The assessment of liver weight revealed no differences between the myocardial I/R and infarction groups (supplemental Table V). This result supports our histological findings and indicates an absence of liver congestion in the myocardial I/R and infarction groups.

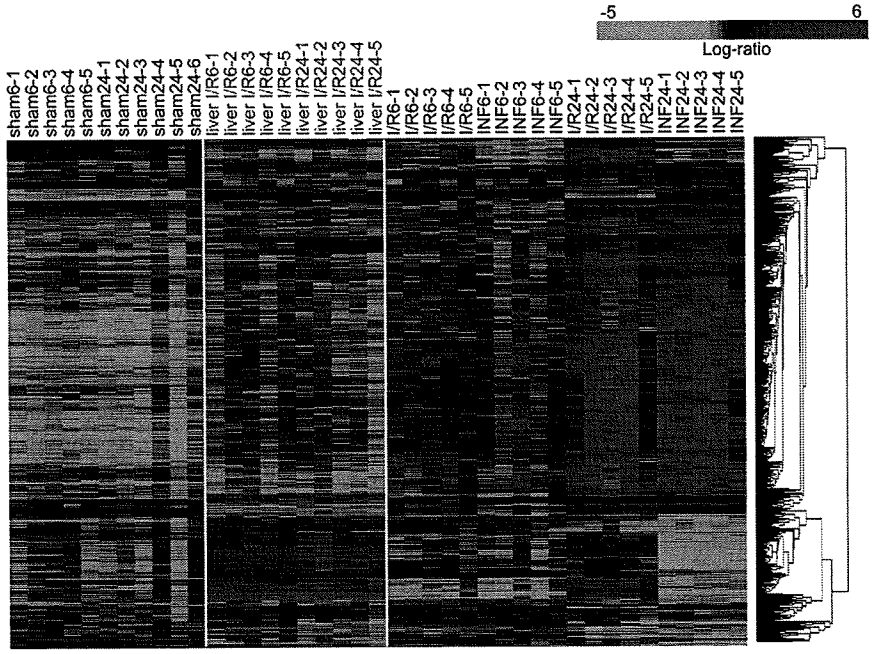

Figure 5. One-way hierarchical clustering and a heat map of the liver I/R group and others with the same extracted genes as shown in Figure 4. Each column corresponds to a sample, and each row represents a gene. The gene cluster data are graphically presented as colored images: red indicates upregulated genes, and green indicates downregulated genes. The genes with the most similar patterns of expression are adjacent to one another. Gene expression patterns induced in the liver I/R group clearly differed from those in the myocardial I/R and infarction groups.

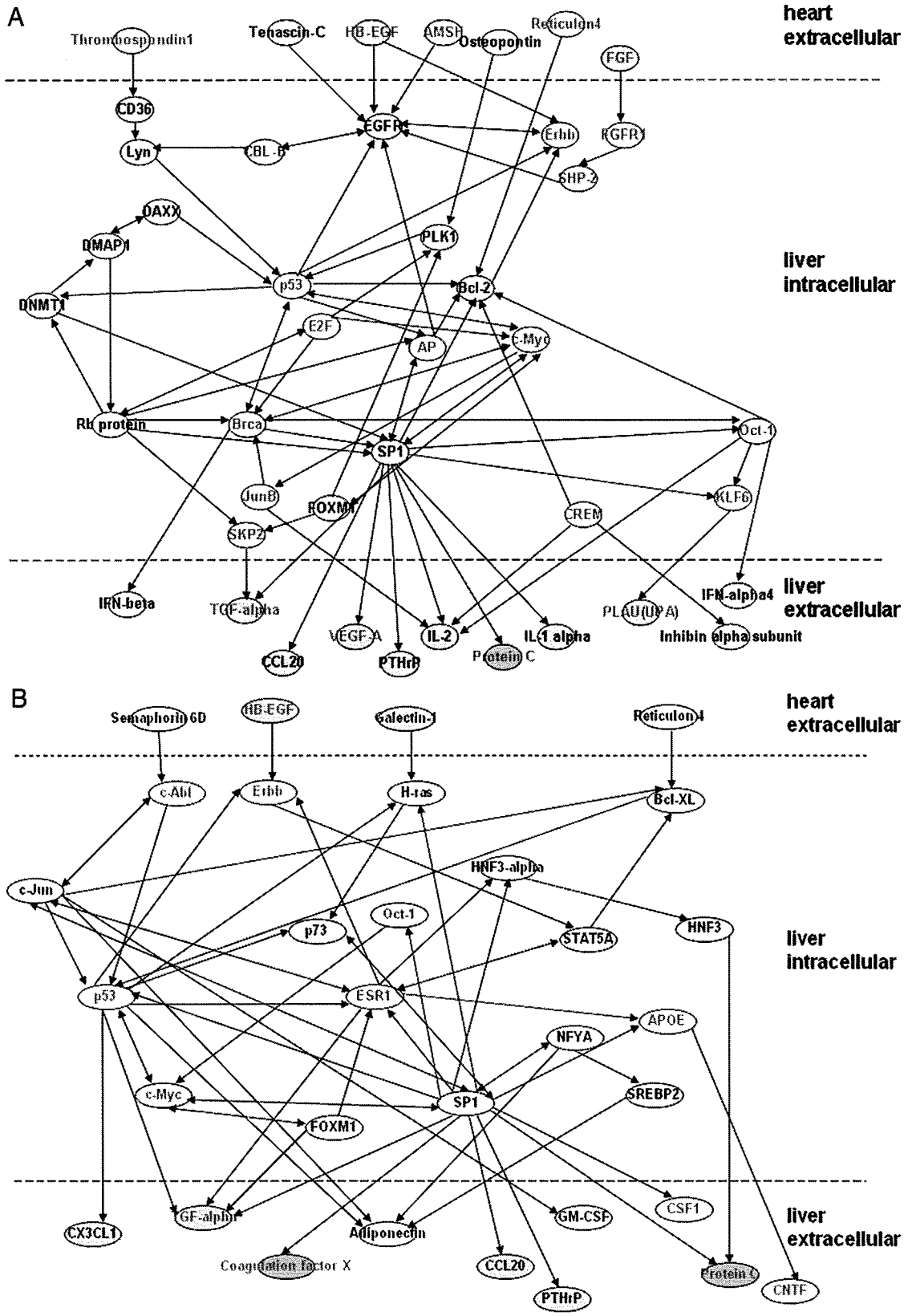

Figure 6. A, Postulated gene network of differentially expressed genes in infarction. B, Postulated gene network of differentially expressed genes in I/R. Detailed definitions of heart-extracellular, liver-intracellular, and liver-extracellular are given in the Methods. Yellow ovals indicate genes related to angiogenesis; green ovals, genes related to coagulation-fibrinolysis; blue ovals, genes related to inflammation; and red characters, genes upregulated in microarray analysis of primary hepatocytes treated with osteopontin. The network diagrams consist of representative genes. All abbreviations are defined in supplemental Tables VI through XI.

Detailed Gene Network Analysis Between the Liver and Heart in Myocardial Ischemia

Several factors can affect the liver, including humoral factors released from the ischemic myocardium, the hemodynamic state, or the autonomic nervous system. We focused on the possibility that humoral factors released from the heart may affect the liver. Cardiac gene expression profiles induced by myocardial ischemia were investigated to identify cardiac genes affecting the liver. To obtain a detailed and comprehensive gene network for the liver and heart, individual data from the liver after 24 hours were integrated with pooled data from the risk area and nonrisk area of the heart. Initially, we divided the heart and liver genes into 3 groups: heart-extracellular, liver-intracellular, and liver-extracellular. To find the network among these induced genes, published results for the interactions of individual genes were integrated with these results by using MetaCore software (GeneGo, St. Joseph, Mich). Direct interactions between individual genes were sought. Genes were excluded according to the following criteria: (1) heart-extracellular, no output signal into liver-intracellular; (2) liver-intracellular, no bidirectional signals; and (3) liver-extracellular, no input signal from liver-intracellular. As expected, the network of these differentially expressed genes involved complex interactions of individual genes; however, representative signaling pathways for MI or I/R injury were identified (Figure 6).

During MI, fibroblast growth factor, osteopontin, and heparin-binding epidermal growth factor-like growth factor (*HB-EGF*) were upregulated in the heart and may have been systemically secreted. Endothelial growth factor receptor and fibroblast growth factor receptor-1 may play important roles in receiving these signals in the liver. Transcription factors such as *p53*, myelocytomatosis oncogene, *trans*-acting transcription factor 1, and octamer-binding transcription factor 1 are important molecules in the regulation of these signaling pathways. Protein C, VEGF-A, and urokinase were expected to be systemically secreted from the liver (supplemental Tables VI through VIII). After infarction, genes involved in inflammation, the coagulation-fibrinolytic system, and angiogenesis showed preferential expression. After I/R, heparin-binding epidermal growth factor was upregulated in the heart and was expected to be systemically secreted. V-*erb*-a erythroblastic leukemia viral oncogene homolog 4 (avian) may play an important role in receiving these signals in the liver. Transcription factors such as *trans*-acting transcription factor 1, *p53*, estrogen receptor-1α, and signal transducer and activator of transcription 5A are potentially important molecules for regulation of these signaling pathways. Protein C, coagulation factor X, ciliary neurotrophic factor, and colony-stimulating factor-1 (macrophage) (*CSF-1*) were expected to be systemically secreted from the liver. In I/R, angiogenesis-related genes were preferentially upregulated (supplemental Tables IX through XI). On comparison of the expression profiles of the heart and liver, genes expressed at significantly higher levels in the heart than in the liver were designated as He, and those expressed at significantly higher levels in the liver than in the heart were designated as Li. Genes expressed in both the heart and liver were described as He/Li (supplemental Tables VIII and XI). In this analysis, most of the factors that were expected to be secreted from the liver induced by I/R and infarction were liver-specific. Most of these genes were not significantly upregulated in the liver I/R groups.

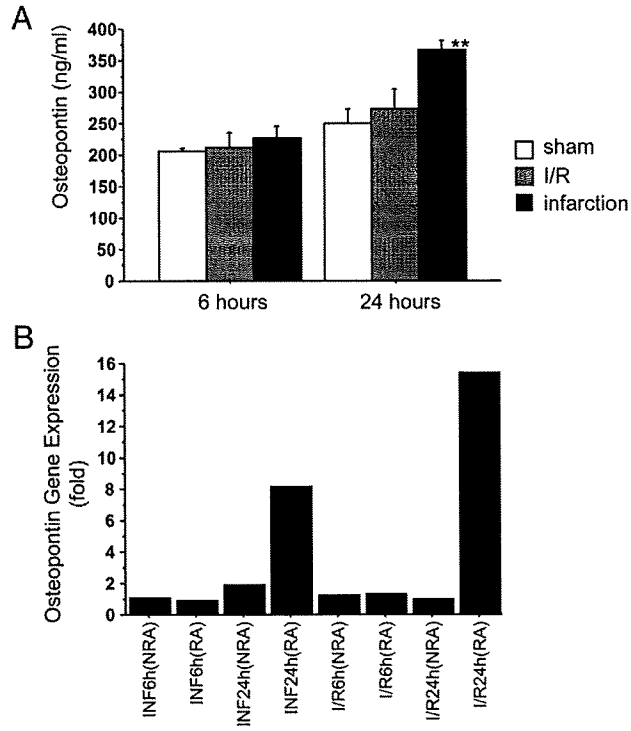

Figure 7. A, The time course of the serum osteopontin concentrations in sham, I/R, and infarction groups. The assessment of serum osteopontin by ELISA in the sham, I/R, and infarction groups after 6 and 24 hours. The serum concentrations of osteopontin after 24 hours were 365.7±14.6 ng/mL, 273.0±30.6 ng/mL, and 249.2±23.4 ng/mL in infarction, I/R, and sham groups, respectively. Error bars represent the SEM. $^{**}P<0.01$ compared with sham. B, The changes in osteopontin gene expression in the infarcted and reperfused heart. INF indicates infarction; NRA, nonrisk area; RA, risk area.

Serum Osteopontin Concentrations in Mice

Of the infarction-induced, cardiac-secreted factors that were expected to stimulate multiple liver genes, we quantified the serum levels of osteopontin by ELISA. Serum osteopontin concentration was significantly increased in the infarction group compared with the sham group ($P=0.0012$) after 24 hours (Figure 7A). In addition, the changes in osteopontin gene expression in the infarcted and reperfused heart are shown in Figure 7B.

Signaling Pathway in Primary Hepatocytes Treated With Osteopontin

To determine whether ischemia-induced, cardiac-secreted factors affected hepatic gene expression, we investigated the effects of osteopontin on primary mouse hepatocytes (supplemental Materials and Methods); 979 genes were upregulated and 734 genes were downregulated ($P<0.05$ and fold change >2.0 determined by class comparison analysis) by osteopontin in primary hepatocytes (GSE14843). The most frequent pathway processes observed among upregulated genes as determined with the use of MetaCore software are

shown in supplemental Table XII. Osteopontin upregulated signaling pathways of protein C, angiogenesis, cell adhesion, etc, which were observed in groups 2 and 3 gene clusters in the mouse liver under conditions of myocardial ischemia (Figure 4; supplemental Tables I and II). The role of osteopontin in the postulated gene network connecting the liver and heart in myocardial ischemia is shown in Figure 6. Interestingly, many of the genes included in the postulated gene network were actually activated by osteopontin ($P<0.05$ or fold change >2.0 by class comparison analysis) in primary hepatocytes. Unexpectedly, osteopontin activated *HB-EGF*, thrombospondin 1, and fibroblast growth factor, which were released from the ischemic heart (Figure 6; supplemental Table VI) in primary hepatocytes. These results indicated that these proteins were released from the liver and from the heart under conditions of myocardial ischemia through osteopontin, and an autocrine signaling pathway may exist in the liver.

Among the candidate hepatic-secreted factors under conditions of myocardial ischemia (Figure 6A; supplemental Table VIII), we quantified the levels of *VEGF-A* in the supernatants of primary hepatocytes treated with osteopontin. The concentration of *VEGF-A* measured by ELISA was significantly increased in the supernatants of primary hepatocytes treated with osteopontin (n=6) compared with the mock group (n=7; $P=0.0042$; supplemental Figure II). Thus, important factors for tissue remodeling could be released from the liver through humoral factors, such as osteopontin, that are released from the heart under conditions of myocardial ischemia.

Quantitative RTD-PCR

We performed a quantitative RTD-PCR with TaqMan probes. In the I/R group, protein C, coagulation factor X, *CNTF*, and *CSF-1* were upregulated in the liver. In the infarction group, protein C, urokinase, and *VEGF-A* were upregulated in the liver (supplemental Figure IIIA). In the hepatocytes treated with osteopontin, protein C, coagulation factor X, ciliary neurotrophic factor, *CSF-1*, urokinase, and *VEGF-A* were upregulated compared with the mock group (supplemental Figure IIIB). These results were consistent with those of cDNA microarray analyses performed in this study.

Discussion

The liver is an essential organ that synthesizes many bioactive proteins, including acute-phase inflammatory proteins (eg, C-reactive protein and IL-6) and coagulation factors. Therefore, it has been speculated that the liver may be involved in systemic reactions that modify the pathophysiology of ACS, although this possibility has not been addressed in detail.

In this study, we examined the gene expression profiles of the livers of mice affected by myocardial I/R or infarction. Marked changes in hepatic gene expression were observed after 24 hours, despite the lack of histological changes in the liver. These changes were essentially restored to normal after 3 to 7 days (data not shown). These findings may not be due to hemodynamic changes during myocardial I/R or infarction. Instead, inflammatory mediators or humoral factors released from the affected heart may be responsible for the observed alterations in hepatic gene expression. This was further confirmed by investigation of signaling pathways in primary hepatocytes induced by osteopontin, a candidate humoral factor released from the ischemic myocardium in vitro.

To exclude the possibility that these changes in gene expression were due to systemic hypotension during I/R or infarction, we performed an additional experiment involving liver I/R to examine whether a pattern of gene expression similar to that in the myocardial I/R and infarction groups could be observed in the liver. Hepatic gene expression in the liver I/R group was completely different from those in the myocardial I/R and infarction groups, with the exception of a small gene cluster (group 3). Although the group 3 gene cluster was upregulated in both the liver I/R and myocardial I/R groups at 24 hours after provocation, peak expression was delayed in the myocardial I/R group compared with the liver I/R group. A recent report of extended observations of cytokine expression in murine hepatic I/R injury indicated that the levels of expression of tumor necrosis factor-α, IL-1β, and IL-6 peaked within 4 hours and returned to baseline at 24 hours.[12] In contrast, in the myocardial I/R and infarction models, these cytokines peaked $\approx$24 to 48 hours and decreased at 7 days.[13] These findings were consistent with those of this study (data not shown). Therefore, the delayed peak of hepatic gene expression observed in this study may be correlated with the extent of inflammation in the myocardium after destruction of myocytes, rather than changes in the hemodynamic state of the liver. The lack of histological changes in the liver in the myocardial I/R and infarction models supported these suggestions, although the influence of hemodynamic state on hepatic gene expression should be carefully considered.

Interestingly, genes related to tissue remodeling, adhesion molecules, and morphogenesis were significantly upregulated in the livers of mice that were subjected to I/R or infarction. This may be related to the induction of tissue repair factors such as angiogenic or myocardiogenic factors in the heart undergoing I/R or infarction. In support of this notion, in addition to the genes upregulated during infarction, chemokines and hormonal factors, including IL-8, androgen, and estrogen receptor genes, were upregulated during I/R. These findings may reflect the presence of living myocytes and the greater release of tissue repair and bioreactive factors during I/R than during infarction.

A recent study that included a sequential analysis of ischemic mouse heart with quantitative RT-PCR demonstrated expression of IL-1β, IL-6, monocyte chemoattractant protein-1, macrophage inflammatory protein-1, and granulocyte-CSF at 6 and 24 hours.[13] These results were essentially consistent with those of our microarray analysis of pooled RNA extracted from heart specimens (data not shown).

In this study, the hepatic RNA samples were not pooled but were used to analyze the hepatic gene expression profiles individually. This strategy was successful, in that our microarray results were consistent with those produced from pooled or nonpooled liver specimens. Moreover, it facilitated the statistical evaluation of differentially expressed genes

among the various groups and revealed dynamic changes in hepatic gene expression through clustering analysis.

We analyzed the network connecting the heart-extracellular genes and liver-intracellular genes induced after I/R injury or infarction by using expression data from pooled heart samples and averaged the expression data for individual liver samples. The results suggested that factors secreted from the heart altered gene expression in the liver. By detailed analysis of signaling pathways, we identified 9 candidate genes (eg, *Osteopontin*, *HB-EGF*, *Reticulon 4*) that were upregulated in the heart and were expected to be systemically secreted and to regulate gene expression in the liver (Figure 6). Moreover, we identified the factors that were expected to be secreted from the liver induced by these signaling pathways, such as protein C, coagulation factor X, *CNTF*, *CSF-1*, and angiogenesis-related genes. These factors were expected to be systemically secreted from the liver and to modulate the pathophysiology and outcome of ACS. It has been reported that protein C prevents myocardial I/R injury,[14] *VEGF* enhances capillary density and improves cardiac function,[15] and urokinase is essential for cardiac functional recovery after acute myocardial infarction.[16]

Of the factors that were expected to be secreted from the heart, we confirmed that infarction increased the serum osteopontin concentration after 24 hours. Osteopontin is essential for the development of myocytes, tissue repair, and angiogenesis, and its downstream products, eg, polo-like kinase, were upregulated in the liver. To confirm these findings, we examined the signaling pathways in primary hepatocytes treated with osteopontin. Osteopontin activated signaling pathways of protein C, angiogenesis, and cell adhesion (supplemental Table XII) by inducing the expression of protein C, urokinase, *VEGF-A*, *CSF-1*, factor X, and ciliary neurotrophic factor (*CNTF*) in primary hepatocytes, which was confirmed by RTD-PCR or ELISA (supplemental Figures II and IIIB). Moreover, many other genes involved in the postulated gene network associating the liver and heart (Figure 6A and 6B) were actually activated in primary hepatocytes treated with osteopontin, confirming this signaling pathway. These results suggest that humoral factors play important roles in signal transduction from the ischemic myocardium to the liver.

Although our results addressed humoral factors from the heart that may affect hepatic gene expression, the effects of other factors, such as autonomic nerves, should also be considered. Because the liver has rich sympathetic and parasympathetic innervation,[17–19] it is possible that sympathetic hyperactivity affects hepatic gene expression. Although hydralazine has been reported to activate sympathetic nerves,[20,21] we observed no differences in gene expression in the hydralazine-treated group compared with the sham-operated group (data not shown). Therefore, autonomic nerves seemed to have little effect on hepatic gene expression determined in this study.

In conclusion, we reported new insights into the pathophysiology of ACS, which may facilitate identification of the mechanisms by which an acute coronary event causes systemic reactions. Further studies are needed to determine whether early therapeutic targeting of the liver during an acute coronary event has any beneficial effect on the clinical outcome in these patients.

Study Limitations

Although we confirmed that the serum osteopontin concentration was increased during myocardial ischemia, other proteins that could potentially be secreted from the heart and liver were not assayed. Further studies are needed to determine whether these proteins, including osteopontin, actually affect hepatic gene expression as observed in this study.

Acknowledgments

We thank Dr Yoh Zen (Department of Human Pathology, Kanazawa University Graduate School of Medical Science, Kanazawa, Japan) for consultation on the pathology of the liver.

Disclosures

None.

References

1. Pfohl M, Schreiber I, Liebich HM, Haring HU, Hoffmeister HM. Upregulation of cholesterol synthesis after acute myocardial infarction—is cholesterol a positive acute phase reactant? *Atherosclerosis.* 1999;142:389–393.
2. Tousoulis D, Antoniades C, Bosinakou E, Kotsopoulou M, Tsoufis C, Marinou K, Charakida M, Stefanadi E, Vavuranakis M, Latsios G, Stefanadis C. Differences in inflammatory and thrombotic markers between unstable angina and acute myocardial infarction. *Int J Cardiol.* 2007;115:203–207.
3. Busch G, Seitz I, Steppich B, Hess S, Eckl R, Schömig A, Ott I. Coagulation factor Xa stimulates interleukin-8 release in endothelial cells and mononuclear leukocytes: implications in acute myocardial infarction. *Arterioscler Thromb Vasc Biol.* 2005;25:461–466.
4. van't Veer LJ, Dai H, van de Vijver MJ, He YD, Hart AA, Mao M, Peterse HL, van der Kooy K, Marton MJ, Witteveen AT, Schreiber GJ, Kerkhoven RM, Roberts C, Linsley PS, Bernards R, Friend SH. Gene expression profiling predicts clinical outcome of breast cancer. *Nature.* 2002;415:530–536.
5. Nielsen TO, West RB, Linn SC, Alter O, Knowling MA, O'Connell JX, Zhu S, Fero M, Sherlock G, Pollack JR, Brown PO, Botstein D, van de Rijn M. Molecular characterization of soft tissue tumours: a gene expression study. *Lancet.* 2002;359:1301–1307.
6. van de Vijver MJ, He YD, van't Veer LJ, Dai H, Hart AA, Voskuil DW, Schreiber GJ, Peterse JL, Roberts C, Marton MJ, Parrish M, Atsma D, Witteveen A, Glas A, Delahaye L, van der Velde T, Bartelink H, Rodenhuis S, Rutgers ET, Friend SH, Bernards R. A gene-expression signature as a predictor of survival in breast cancer. *N Engl J Med.* 2002;347:1999–2009.
7. Hedenfalk I, Duggan D, Chen Y, Radmacher M, Bittner M, Simon R, Meltzer P, Gusterson B, Esteller M, Kallioniemi OP, Wilfond B, Borg A, Trent J, Raffeld M, Yakhini Z, Ben-Dor A, Dougherty E, Kononen J, Bubendorf L, Fehrle W, Pittaluga S, Gruvberger S, Loman N, Johannsson O, Olsson H, Sauter G. Gene-expression profiles in hereditary breast cancer. *N Engl J Med.* 2001;344:539–548.
8. Gabrielsen A, Lawler PR, Yongzhong W, Steinbrüchel D, Blagoja D, Paulsson-Berne G, Kastrup J, Hansson GK. Gene expression signals involved in ischemic injury, extracellular matrix composition and fibrosis defined by global mRNA profiling of the human left ventricular myocardium. *J Mol Cell Cardiol.* 2007;42:870–883.
9. LaFramboise WA, Bombach KL, Dhir RJ, Muha N, Cullen RF, Pogozelski AR, Turk D, George JD, Guthrie RD, Magovern JA. Molecular dynamics of the compensatory response to myocardial infarct. *J Mol Cell Cardiol.* 2005;38:103–117.
10. Giesen PL, Peltenburg HG, de Zwaan C, Janson PC, Flendrig JG, Hermens WT. Greater than expected alanine aminotransferase activities in plasma and in hearts of patients with acute myocardial infarction. *Clin Chem.* 1989;35:279–283.
11. Lu J, Getz G, Miska EA, Alvarez-Saavedra E, Lamb J, Peck D, Sweet-Cordero A, Ebert BL, Mak RH, Ferrando AA, Downing JR, Jacks T, Horvitz HR, Golub TR. MicroRNA expression profiles classify human cancers. *Nature.* 2005;435:834–838.
12. Langdale LA, Hoagland V, Benz W, Riehle KJ, Campbell JS, Liggitt DH, Fausto N. Suppressor of cytokine signaling expression with increasing

severity of murine hepatic ischemia-reperfusion injury. *J Hepatol.* 2008; 49:198–206.
13. Vandervelde S, van Luyn MJ, Rozenbaum MH, Petersen AH, Tio RA, Harmsen MC. Stem cell-related cardiac gene expression early after murine myocardial infarction. *Cardiovasc Res.* 2007;73:783–793.
14. Loubele ST, Spek CA, Leenders P, van Oerle R, Aberson HL, Hamulyák K, Ferrell G, Esmon CT, Spronk HM, ten Cate H. Activated protein C protects against myocardial ischemia/reperfusion injury via inhibition of apoptosis and inflammation. *Arterioscler Thromb Vasc Biol.* 2009;29: 1087–1092.
15. Zhang J, Ding L, Zhao Y, Sun W, Chen B, Lin H, Wang X, Zhang L, Xu B, Dai J. Collagen-targeting vascular endothelial growth factor improves cardiac performance after myocardial infarction. *Circulation.* 2009;119: 1776–1784.
16. Heymans S, Luttun A, Nuyens D, Theilmeier G, Creemers E, Moons L, Dyspersin GD, Cleutjens JP, Shipley M, Angellilo A, Levi M, Nübe O, Baker A, Keshet E, Lupu F, Herbert JM, Smits JF, Shapiro SD, Baes M, Borgers M, Collen D, Daemen MJ, Carmeliet P. Inhibition of plasminogen activators or matrix metalloproteinases prevents cardiac rupture but impairs therapeutic angiogenesis and causes cardiac failure. *Nat Med.* 1999;5:1135–1142.
17. Sasse D, Spornitz UM, Maly IP. Liver architecture. *Enzyme.* 1992; 46:8–32.
18. McCuskey RS, Reilly FD. Hepatic microvasculature: dynamic structure and its regulation. *Semin Liver Dis.* 1993;13:1–12.
19. Berthoud HR. Anatomy and function of sensory hepatic nerves. *Anat Rec A Discov Mol Cell Evol Biol.* 2004;280:827–835.
20. Yoshioka M, Togashi H, Minami M, Saito H. Effects of hydralazine on adrenal and cardiac sympathetic nerve activity in anesthetized rats. *Res Commun Chem Pathol Pharmacol.* 1986;54:313–320.
21. Johansson M, Elam M, Rundqvist B, Eisenhofer G, Herlitz H, Jensen G, Friberg P. Differentiated response of the sympathetic nervous system to angiotensin-converting enzyme inhibition in hypertension. *Hypertension.* 2000;36:543–548.

CLINICAL PERSPECTIVE

Acute coronary syndrome (ACS) is accompanied by systemic changes in inflammation, coagulation, and metabolism, which may affect the outcome and prognosis of ACS. These systemic reactions are not explained by cardiac events alone. Several lines of evidence suggest that patients with fatty liver disease have a high risk of developing cardiovascular diseases, and it is possible to speculate that the liver is involved in a systemic reaction that modifies the pathogenesis of ACS. However, the relation between liver and myocardial ischemia in the acute ischemic phase has not been elucidated so far. In this investigation, we simultaneously analyzed the gene expression profiles of the liver and heart during acute myocardial ischemia in mice and observed the presence of humoral factors that intervened between the heart and liver. These humoral factors were released from the heart and influenced the liver to secrete important tissue remodeling factors. One of these humoral factors, osteopontin, a widely expressed glycoprotein, was increased in the ischemic heart and altered the gene expression of hepatocytes to produce important tissue remodeling factors (such as vascular endothelial growth factor-A). Our observations suggest that hepatic gene expression is potentially regulated by humoral factors of cardiac origin provoked by myocardial ischemia, and we provide direct evidence that the liver is involved in a systemic reaction that accompanies ACS. Our findings provide potential new insights into the pathophysiology of ACS.

nature genetics

Genome-wide association of *IL28B* with response to pegylated interferon-α and ribavirin therapy for chronic hepatitis C

Yasuhito Tanaka[1,18], Nao Nishida[2,18], Masaya Sugiyama[1], Masayuki Kurosaki[3], Kentaro Matsuura[1], Naoya Sakamoto[4], Mina Nakagawa[4], Masaaki Korenaga[5], Keisuke Hino[5], Shuhei Hige[6], Yoshito Ito[7], Eiji Mita[8], Eiji Tanaka[9], Satoshi Mochida[10], Yoshikazu Murawaki[11], Masao Honda[12], Akito Sakai[12], Yoichi Hiasa[13], Shuhei Nishiguchi[14], Asako Koike[15], Isao Sakaida[16], Masatoshi Imamura[17], Kiyoaki Ito[17], Koji Yano[17], Naohiko Masaki[17], Fuminaka Sugauchi[1], Namiki Izumi[3], Katsushi Tokunaga[2] & Masashi Mizokami[1,17]

The recommended treatment for patients with chronic hepatitis C, pegylated interferon-α (PEG-IFN-α) plus ribavirin (RBV), does not provide sustained virologic response (SVR) in all patients. We report a genome-wide association study (GWAS) to null virological response (NVR) in the treatment of patients with hepatitis C virus (HCV) genotype 1 within a Japanese population. We found two SNPs near the gene *IL28B* on chromosome 19 to be strongly associated with NVR (rs12980275, $P = 1.93 \times 10^{-13}$, and rs8099917, 3.11×10^{-15}). We replicated these associations in an independent cohort (combined *P* values, 2.84×10^{-27} (OR = 17.7; 95% CI = 10.0–31.3) and 2.68×10^{-32} (OR = 27.1; 95% CI = 14.6–50.3), respectively). Compared to NVR, these SNPs were also associated with SVR (rs12980275, $P = 3.99 \times 10^{-24}$, and rs8099917, $P = 1.11 \times 10^{-27}$). In further fine mapping of the region, seven SNPs (rs8105790, rs11881222, rs8103142, rs28416813, rs4803219, rs8099917 and rs7248668) located in the *IL28B* region showed the most significant associations ($P = 5.52 \times 10^{-28}$–2.68×10^{-32}; OR = 22.3–27.1). Real-time quantitative PCR assays in peripheral blood mononuclear cells showed lower *IL28B* expression levels in individuals carrying the minor alleles ($P = 0.015$).

Hepatitis C is a global health problem that affects a significant proportion of the world's population. The World Health Organization estimated that in 1999, there were 170 million HCV carriers worldwide, with 3–4 million new cases appearing each year. HCV infection affects more than 4 million people in the United States, where it represents the leading cause of cirrhosis and hepatocellular carcinoma as well as the leading cause of liver transplantation[1].The American Gastroenterological Association estimated that drugs are the largest direct costs of hepatitis C[1].

The most effective current standard of care in patients with chronic hepatitis C, a combination of PEG-IFN-α with ribavirin, does not produce SVR in all patients treated. Large-scale studies on 48-week-long PEG-IFN-α/RBV treatment in the United States and Europe showed that 42–52% of patients with HCV genotype 1 achieved SVR[2–4], and similar results were found in Japan. However, older patients (greater than 50 years of age) had a significantly lower rate of SVR due to poor adherence resulting from adverse events and laboratory-detectable abnormalities such as neutropenia and thrombocytopenia[5,6]. Specifically, various well-described side effects (such as a flu-like syndrome, hematologic abnormalities and adverse neuropsychiatric events) often necessitate dose reduction, and 10–14% of patients require premature withdrawal from interferon-based therapy[7]. To avoid these side effects in patients who will not be helped by the treatment, as well as to reduce the substantial cost of PEG-IFN-α/RBV treatment, it would be useful to be able to predict an individual's response before or early in treatment. Several viral factors, such as genotype 1, high baseline viral load, viral

[1]Department of Clinical Molecular Informative Medicine, Nagoya City University Graduate School of Medical Sciences, Nagoya, Japan. [2]Department of Human Genetics, Graduate School of Medicine, The University of Tokyo, Tokyo, Japan. [3]Division of Gastroenterology and Hepatology, Musashino Red Cross Hospital, Tokyo, Japan. [4]Department of Gastroenterology and Hepatology, Tokyo Medical and Dental University, Tokyo, Japan. [5]Division of Hepatology and Pancreatology, Kawasaki Medical College, 577 Matsushima, Kurashiki, Japan. [6]Department of Internal Medicine, Hokkaido University Graduate School of Medicine, Sapporo, Japan. [7]Molecular Gastroenterology and Hepatology, Kyoto Prefectural University of Medicine, Kyoto, Japan. [8]National Hospital Organization Osaka National Hospital, Osaka, Japan. [9]Department of Medicine, Shinshu University School of Medicine, Matsumoto, Japan. [10]Division of Gastroenterology and Hepatology, Internal Medicine, Saitama Medical University, Saitama, Japan. [11]Second department of Internal Medicine, Faculty of Medicine, Tottori University, Yonago, Japan. [12]Department of Gastroenterology, Kanazawa University Graduate School of Medicine, Kanazawa, Japan. [13]Department of Gastroenterology and Metabology, Ehime University Graduate School of Medicine, Ehime, Japan. [14]Department of Internal Medicine, Hyogo College of Medicine, Nishinomiya, Japan. [15]Central Research Laboratory, Hitachi Ltd., Kokubunji, Japan. [16]Gastroenterology and Hepatology, Yamaguchi University Graduate School of Medicine, Yamaguchi, Japan. [17]Research Center for Hepatitis and Immunology, International Medical Center of Japan Konodai Hospital, Ichikawa, Japan. [18]These authors contributed equally to this work. Correspondence should be addressed to M.M. (mmizokami@imcjk2.hosp.go.jp).

Received 29 June; accepted 21 August; published online 13 September 2009; doi:10.1038/ng.449

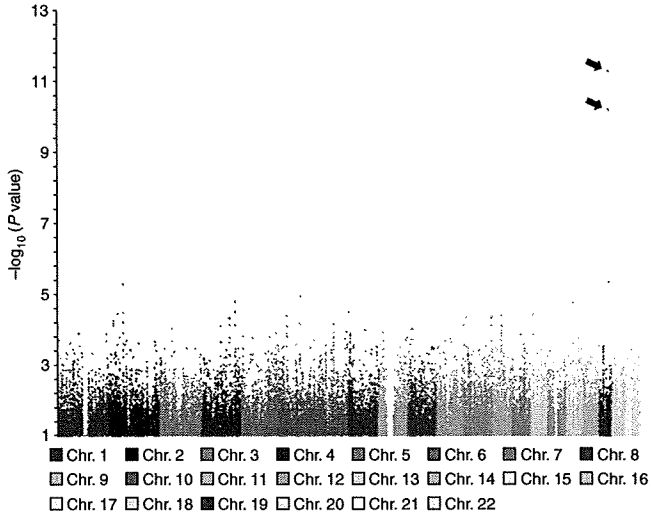

Figure 1 Genome-wide association results with PEG-IFN-α/RBV treatment in 142 Japanese patients with HCV (78 NVR and 64 VR samples). *P* values were calculated by using a χ^2 test for allele frequencies. The dots with arrows for chromosome 19 denote SNPs that showed significant genome-wide associations ($P < 8.05 \times 10^{-8}$) with response to PEG-IFN-α/RBV treatment.

kinetics during treatment, and amino acid pattern in the interferon sensitivity–determining region, have been reported to be significantly associated with the treatment outcome in a number of independent studies[8–10]. Studies have also provided strong evidence that ~20% of patients with HCV genotype 1 and 5% of patients with genotype 2 or 3 have a null response to PEG-IFN-α/RBV. No definite predictor of this resistance is currently available that make it possible to bypass the initial 12–24 weeks' treatment before deciding whether treatment should be continued. If a reliable predictor of non-response were identified for use in patients before treatment initiation, then an estimated 20%, including those who have little or no chance to achieve SVR, could be spared the side effects and cost of treatment.

Host factors, including age, sex, race, liver fibrosis and obesity, have also been reported to be associated with PEG-IFN-α/RBV therapy outcome[11,12]. However, little is known about the host genetic factors that might be associated with the response to therapy: thus far only a few candidate genes, including those encoding type I interferon receptor-1 (*IFNAR1*) and mitogen-activated protein kinase–activated protein kinase 3 (*MAPKAPK3*), have been reported to be associated with treatment response[13,14]. We describe here a GWAS for response to PEG-IFN-α/RBV treatment.

We conducted this GWAS to identify host genes associated with response to PEG-IFN-α/RBV treatment in 154 Japanese patients with HCV genotype 1 (82 with NVR and 72 with virologic response (VR), based on the selection criteria as described in Online Methods). We used the Affymetrix SNP 6.0 genome-wide SNP typing array for 900,000 SNPs. A total of 621,220 SNPs met the following criteria: (i) SNP call rate ≥95%, (ii) minor allele frequency (MAF) ≥1% and (iii) deviation from Hardy-Weinberg equilibrium (HWE) $P \geq 0.001$ in VR samples. After excluding 4 NVR and 8 VR samples that showed quality control (QC) call rates of <95%, 78 NVR and 64 VR samples were included in the association analysis. **Figure 1** shows a genome-wide view of the single-point association data based on allele frequencies. Two SNPs located close to *IL28B* on chromosome 19 showed strong associations, with a minor allele dominant model (rs12980275, $P = 1.93 \times 10^{-13}$, and rs8099917, $P = 3.11 \times 10^{-15}$, respectively), with NVR to PEG-IFN-α/RBV treatment (**Table 1**). The rs8099917 lies between *IL28B* and *IL28A*, ~8 kb downstream from *IL28B* and ~16 kb upstream from *IL28A*. These associations reached genome-wide levels of significance for both SNPs in this initial GWAS cohort (Bonferroni criterion $P < 8.05 \times 10^{-8}$ (0.05/621,220)). The frequencies of minor allele–positive patients were much higher in the NVR group than in the VR group for both SNPs (74.3% in NVR, 12.5% in VR for rs12980275; 75.6% in NVR, 9.4% in VR for rs8099917). Notably, individuals homozygous for the minor allele were observed only in the NVR group. The VR group, as compared to the NVR group, showed genotype frequencies closer to those in the healthy Japanese population[15], yet the minor allele frequencies were slightly higher in the transient virologic response (TVR) group (23.1%, 15.4%) than in the SVR group (9.8%, 7.8%) (**Table 1**). We applied the Cochrane-Armitage test on all the SNPs and found a genetic inflation factor, λ, of 1.029 for the GWAS stage (**Supplementary Fig. 1**). We also carried out principal component analysis in 142 samples for the GWAS stage together with the HapMap samples (CEU, YRI, CHB and JPT) (**Supplementary Fig. 2**); this suggested that the effect of population stratification was negligible.

Table 1 Significant association of two SNPs (rs12980275 and rs8099917) with response to PEG-IFN-α/RBV treatment

					Null responder (NVR[a], *n* = 128)			Responder (VR[a], *n* = 186)			Responder (SVR[a], *n* = 140)			NVR vs. VR		NVR vs. SVR	
dbSNP rsID	Nearest gene	MAF[b] (allele)	Allele (1/2)	Stage	11	12	22	11	12	22	11	12	22	OR (95% CI)[c]	*P* value[d]	OR (95% CI)[c]	*P* value[d]
rs12980275	*IL28B*	0.15 (G)	A/G	GWAS	20 (25.6)	54 (69.2)	4 (5.1)	56 (87.5)	8 (12.5)	0 (0.0)	46 (90.2)	5 (9.8)	0 (0.0)	20.3 (8.3–49.9)	1.93×10^{-13}	26.7 (9.3–76.5)	7.41×10^{-13}
				Replication	10 (20.0)	37 (74.0)	3 (6.0)	101 (82.8)	21 (17.2)	0 (0.0)	73 (82.0)	16 (18.0)	0 (0.0)	19.2 (8.3–44.4)	5.46×10^{-15}	18.3 (7.6–44.0)	8.37×10^{-13}
				Combined	30 (23.4)	91 (71.1)	7 (5.5)	157 (84.4)	29 (15.6)	0 (0.0)	119 (85.0)	21 (15.0)	0 (0.0)	17.7 (10.0–31.3)	2.84×10^{-27}	18.5 (10.0–34.4)	3.99×10^{-24}
rs8099917	*IL28B*	0.12 (G)	T/G	GWAS	19 (24.4)	56 (71.8)	3 (3.8)	58 (90.6)	6 (9.4)	0 (0.0)	47 (92.2)	4 (7.8)	0 (0.0)	30.0 (11.2–80.5)	3.11×10^{-15}	36.5 (11.6–114.6)	5.00×10^{-14}
				Replication	11 (22.0)	37 (74.0)	2 (4.0)	108 (88.5)	14 (11.5)	0 (0.0)	78 (87.6)	11 (12.4)	0 (0.0)	27.4 (11.5–65.3)	9.47×10^{-18}	25.1 (10.0–63.1)	1.00×10^{-14}
				Combined	30 (23.4)	93 (72.7)	5 (3.9)	166 (89.2)	20 (10.8)	0 (0.0)	125 (89.3)	15 (10.7)	0 (0.0)	27.1 (14.6–50.3)	2.68×10^{-32}	27.2 (13.9–53.4)	1.11×10^{-27}

[a]NVR, null virologic response; VR, virologic response; SVR, sustained virologic response. The 186 VRs consisted of 46 transient virologic response (TVRs) and 140 SVRs. [b]Minor allele frequency and minor allele in 184 healthy Japanese individuals[15]. The MAF of the SNPs in SVR is similar to that of TVR group, whereas that of NVR is much higher (76.6%). [c]Odds ratio for the minor allele in a dominant model. [d]*P* value by χ^2 test for the minor allele dominant model.

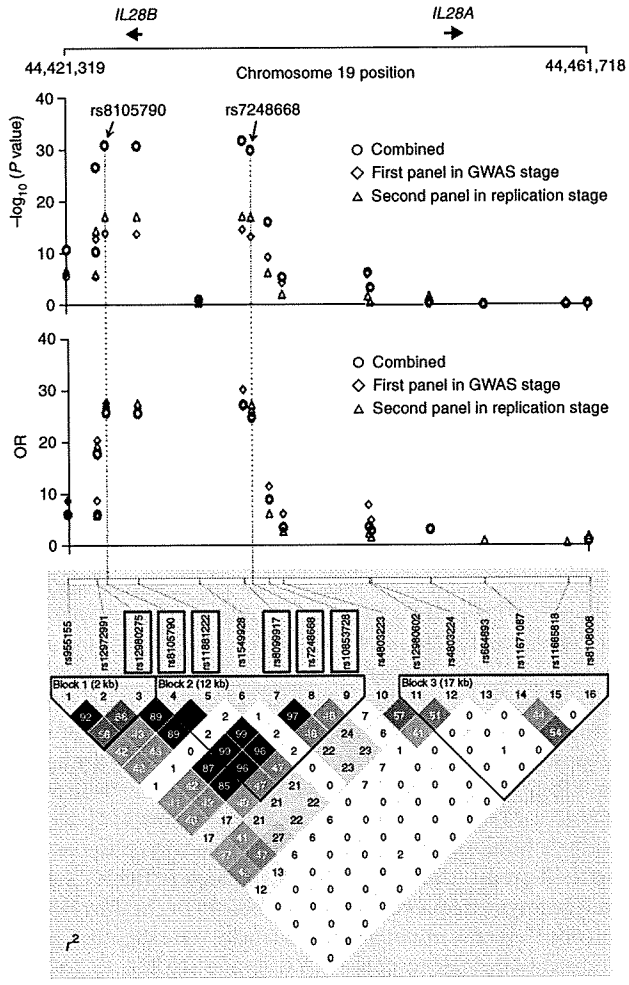

Figure 2 Genomic structure, *P* value and OR plots in association analysis and LD map around *IL28B* and *IL28A* (chr.19, nucleotide positions 44421319–44461718; build 35). *P* values by the χ^2 test for minor allele dominant effect model are shown for the first panel of 142 samples in the GWAS stage, the second panel of 172 samples in the replication stage, and the combined analysis. Below are estimates of pairwise r^2 for 16 SNPs selected in the replication study using a total of 314 Japanese patients with HCV treated with PEG-IFN-α/RBV. Boxes indicate the significantly associated SNPs with response to PEG-IFN-α/RBV treatment both in the GWAS stage and in the replication stage. Dotted lines indicate the region with the strongest associations from the positions of rs8105790 to rs7248668.

We analyzed the region of ~40 kb (chr. 19, nucleotide positions 44421319–44461718; build 35) containing the significantly associated SNPs (rs12980275 and rs8099917) using Haploview software for linkage disequilibrium (LD) and haplotype structure based on the HapMap data for individuals of Japanese ancestry. The LD blocks were analyzed using the four-gamete rule, and four blocks were observed (**Supplementary Fig. 3**). We selected 16 SNPs for both replication study and high-density association mapping, including tagging SNPs estimated on the basis of the haplotype blocks, one SNP located within *IL28B* (rs11881222) and the significantly associated SNPs from the GWAS stage (rs12980275 and rs8099917) (**Supplementary Table 1**).

To validate the results of the GWAS stage, 16 SNPs selected for the replication stage, including the original SNPs, were genotyped using the DigiTag2 assay in an independent set of 172 Japanese patients with HCV treated with PEG-IFN-α/RBV treatment (50 NVR and 122 VR samples), together with the first panel of 142 samples analyzed in the GWAS stage (**Supplementary Table 1**). The associations of the original SNPs were replicated in the replication cohort of 172 patients ($P = 5.46 \times 10^{-15}$, OR = 19.2 for rs12980275; $P = 9.47 \times 10^{-18}$, OR = 27.4 for rs8099917; **Table 1**). The combined *P* values for both stages reached 2.84×10^{-27} (OR = 17.7; 95% CI = 10.0–31.3) and 2.68×10^{-32} (OR = 27.1; 95% CI = 14.6–50.3), respectively (**Table 1**). Notably, when we compared the SVR ($n = 140$) with the NVR group ($n = 128$), the original two SNPs (rs12980275 and rs8099917) again showed strong associations: both *P* values and ORs were similar to those observed in the comparison between VR and NVR, and the combined *P* values for both stages reached 3.99×10^{-24} (OR = 18.5; 95% CI = 10.0–34.4) and 1.11×10^{-27} (OR = 27.2; 95% CI = 13.9–53.4), respectively (**Table 1**). Comparing SVR ($n = 140$) versus NVR plus TVR ($n = 174$), we again found that these SNPs were significantly associated ($P = 1.71 \times 10^{-16}$, OR = 8.8; 95% CI 5.1–15.4 for rs12980275; $P = 1.18 \times 10^{-18}$, OR = 12.1; 95% CI 6.5–22.4 for rs8099917, **Supplementary Table 2**), suggesting that these SNPs would predict NVR as well as SVR before PEG-IFN-α/RBV therapy.

Among the newly analyzed SNPs in the replication study, six (rs12980275, rs8105790, rs11881222, rs8099917, rs7248668 and rs10853728) showed significant associations both in the GWAS stage ($P < 8.05 \times 10^{-8}$) and in the replication stage ($P < 0.0031$ (0.05/16)) after Bonferroni correction. These SNPs are located within a 15.7-kb region that includes *IL28B* (**Fig. 2** and **Supplementary Table 1**). In particular, the strongest associations with NVR were observed for four SNPs, rs8105790, rs11881222, rs8099917 and rs7248668, that are located in the downstream flanking region, the third intron and the upstream flanking region of *IL28B*. The combined *P* values for these polymorphisms were 1.98×10^{-31} (OR = 25.7; 95% CI = 13.9–47.6), 2.84×10^{-31} (OR = 25.6; 95% CI = 13.8–47.3), 2.68×10^{-32} (OR = 27.1; 95% CI = 14.6–50.3) and 1.84×10^{-30} (OR = 24.7; 95% CI = 13.3–45.8), respectively (**Supplementary Table 1**). We then sequenced this region to identify further variants and found three SNPs (rs8103142, rs28416813 and rs4803219) located in the third exon, the first intron and the upstream flanking region of *IL28B*, and a few infrequent variations. These SNPs also showed strong associations in the combined dataset of 128 NVR and 186 VR samples ($P = 1.40 \times 10^{-29}$, OR = 26.6 for rs8103142; $P = 5.52 \times 10^{-28}$, OR = 22.3 for rs28416813; $P = 2.45 \times 10^{-29}$, OR = 23.3 for rs4803219; **Supplementary Table 3**). We also performed LD and haplotype analyses with seven SNPs. These SNPs were in strong LD, and the risk haplotype showed a level of association similar to those of individual SNPs ($P = 1.35 \times 10^{-25}$, OR = 11.1; 95% CI = 6.6–18.6) (**Table 2**). These results suggest that the association with NVR was primarily driven by one of these SNPs.

Table 2 Association analysis of response to treatment by *IL28B* haplotype

SNP							Frequencies			
rs8105790	rs11881222	rs8103142	rs28416813	rs4803219	rs8099917	rs7248668	NVR group	VR group	*P* value	OR (95% CI)
T	A	T	C	C	T	G	0.543	0.942	1.81×10^{-32}	0.1 (0.04–0.12)
C	G	C	G	T	G	A	0.387	0.054	1.35×10^{-25}	11.1 (6.6–18.6)

Association analysis of haplotypes consisting of seven SNPs with response to PEG-IFN-α/RBV treatment in 314 Japanese patients with HCV. Boldface letters: rs11881222 (third intron); rs8103142 (third exon).

Table 3 Factors associated with NVR by logistic regression model

Factors	Odds ratio	95% CI	*P* value
rs8099917 (G allele)	37.68	16.71–83.85	<0.0001
Age	1.02	0.98–1.07	0.292
Gender (Female)	3.32	1.49–7.39	0.003
Re-treatment[a]	1.12	0.55–2.33	0.750
Platelet count	0.93	0.87–1.01	0.080
Aminotransferase level	1.00	0.99–1.00	0.735
Fibrosis stage[20]	1.10	0.73–1.66	0.658
HCV-RNA level	1.01	0.99–1.02	0.139

[a]Re-treatment, non-response to previous treatment with interferon-α (plus RBV).

To examine the relative contribution of factors associated with NVR, we used a logistic regression model. One tagging SNP located within *IL28B* (minor allele of rs8099917) was the most significant factor for predicting NVR, followed by gender (**Table 3**). Clinically, viral factors such as HCV genotype and HCV RNA level are important for the outcome of PEG-IFN-α/RBV therapy. Indeed, mean HCV-RNA level was significantly lower in SVR (SVR versus TVR, $P = 0.002$; SVR versus NVR, $P = 0.016$; **Supplementary Table 4**). Mean platelet count and the proportion of mild fibrosis (F1–F2) were significantly higher in SVR than in NVR.

Real-time quantitative PCR assays in peripheral blood mononuclear cells revealed a significantly lower level of *IL28* mRNA expression in individuals with the minor alleles (**Fig. 3**), suggesting that variant(s) regulating *IL28* expression is associated with a response to PEG-IFN-α/RBV treatment. *IL28B* encodes a cytokine distantly related to type I (α and β) interferons and the interleukin (IL)-10 family. This gene and *IL28A* and *IL29* (encoding IL-28A and IL-29, respectively) are three closely related cytokine genes that encode proteins known as type III IFNs (IFN-λs) and that form a cytokine gene cluster at chromosomal region 19q13 (ref. 16). The three cytokines are induced by viral infection and have antiviral activity[16,17]. All three interact with a heterodimeric class II cytokine receptor that consists of IL-10 receptor beta (IL10Rβ) and IL-28 receptor alpha (IL28Rα, encoded by *IL28RA*)[16,17], and they may serve as an alternative to type I IFNs in providing immunity to viral infection.

Notably, a recent report showed that the strong antiviral activity evoked by treating mice with TLR3 or TLR9 agonists was significantly reduced in both *IL28RA*$^{-/-}$ and *IFNAR*$^{-/-}$ mice, indicating that IFN-λ is important in mediating antiviral protection by ligands for TLR3 and TRL9 (ref. 18). IFN-λ induced a steady increase in the expression of a subset of IFN-stimulated genes, whereas IFN-α induced the same genes with more rapid and transient kinetics[19]. Therefore, it is possible that IFN-λ induces a slower but more sustained response that is important for TLR-mediated antiviral protection. This might be one of the ways that a genetic variant regulating *IL28* expression influences the response to PEG-IFN-α/RBV treatment. Further research will be required to fully understand the specific mechanism by which a genotype might affect the response to treatment.

In conclusion, the strongest associations with NVR were observed for seven SNPs, rs8105790, rs11881222, rs8103142, rs28416813, rs4803219, rs8099917 and rs7248668, that are located in the downstream flanking region, the third intron, the third exon, the first intron and the upstream flanking region of *IL28B*. Further studies following our report of this robust genetic association to NVR may make it possible to develop a pre-treatment predictor of which individuals are likely to respond to PEG-IFN-α/RBV treatment. This would remove the need for the initial 12–24 weeks of treatment that is currently used as a basis for a clinical decision about whether treatment should be continued. That would allow better targeting of PEG-IFN-α/RBV treatment, avoiding the unpleasant side effects that commonly accompany the treatment where it is unlikely to be beneficial, and reduce overall treatment costs. Because of the small number of samples in this study, we plan to conduct a further prospective multicenter study to establish these SNPs as a clinically useful marker.

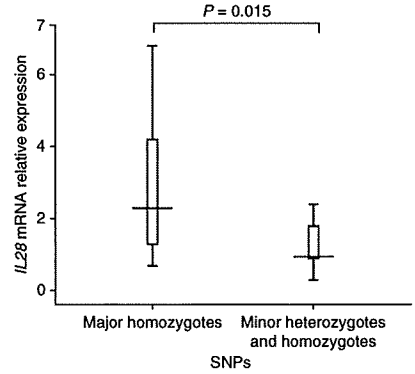

Figure 3 Quantification of *IL28* mRNA expression. The expression level of *IL28* genes was determined by real-time quantitative RT-PCR using RNA purified from peripheral blood mononuclear cells. Distribution of relative gene expression levels was compared between the individuals homozygous for major alleles ($n = 10$) and the heterozygous or homozygous individuals carrying minor alleles ($n = 10$) of rs8099917 by using the Mann-Whitney *U*-test. The bars indicate the median. All samples were obtained from HCV-infected patients before PEG-IFN-α/RBV therapy.

METHODS

Methods and any associated references are available in the online version of the paper at http://www.nature.com/naturegenetics/.

Note: Supplementary information is available on the Nature Genetics website.

ACKNOWLEDGMENTS

This study was supported by a grant-in-aid from the Ministry of Health, Labour, and Welfare of Japan (H19-kannen-013). This study is based on 15 multicenter hospitals throughout Japan, in the Hokkaido area (Hokkaido University Hospital), Kanto area (Saitama University Hospital; Konodai Hospital; Musashino Red Cross Hospital; Tokyo Medical and Dental University Hospital), Koshin area (Shinshu University Hospital; Kanazawa University Hospital), Tokai area (Nagoya City University Hospital), Kinki area (Kyoto Prefectural University of Medicine Hospital; National Hospital Organization Osaka National Hospital; Hyogo College of Medicine Hospital) and Chugoku/Shikoku area (Tottori University Hospital; Ehime University Hospital; Yamaguchi University Hospital; Kawasaki Medical College Hospital). We thank Y. Uehara-Shibata, Y. Ogasawara, Y. Ishibashi and M. Yamaoka-Sageshima (Tokyo University) for technical assistance; A. Matsumoto (Shinshu), K. Naiki (Saitama), K. Nishimura (Kyoto), H. Enomoto (Hyogo), K. Oyama (Tottori) and the Ochanomizu Liver Conference Study Group for collecting samples; M. Watanabe (Tokyo Medical and Dental University), S. Kaneko (Kanazawa University) and M. Onji (Ehime University) for their advice throughout the study; and H. Ito (Aichi Cancer Center) for conducting statistical analyses.

AUTHOR CONTRIBUTIONS

Study design and discussion: Y.T., N.N., N.M., K.T., M.M.; sample collection: Y.T., M.K., K.M., N.S., M.N., M.K., K.H., S.H., Y.I., E.M., E.T., S.M., Y.M., M.H., A.S., Y.H., S.N., I.S., M.I., K.I., K.Y., F.S., N.I.; genotyping: N.N.; statistical analysis: N.N., A.K., K.I.; quantitative RT-PCR: M.S.; manuscript writing: Y.T., N.N., K.T., M.M.

Published online at http://www.nature.com/naturegenetics/.
Reprints and permissions information is available online at http://npg.nature.com/reprintsandpermissions/.

1. Ray Kim, W. Global epidemiology and burden of hepatitis C. *Microbes Infect.* **4**, 1219–1225 (2002).
2. Manns, M.P. *et al.* Peginterferon alfa-2b plus ribavirin compared with interferon alfa-2b plus ribavirin for initial treatment of chronic hepatitis C: a randomised trial. *Lancet* **358**, 958–965 (2001).

3. Fried, M.W. *et al.* Peginterferon alfa-2a plus ribavirin for chronic hepatitis C virus infection. *N. Engl. J. Med.* **347**, 975–982 (2002).
4. Hadziyannis, S.J. *et al.* Peginterferon-alpha2a and ribavirin combination therapy in chronic hepatitis C: a randomized study of treatment duration and ribavirin dose. *Ann. Intern. Med.* **140**, 346–355 (2004).
5. Bruno, S. *et al.* Peginterferon alfa-2b plus ribavirin for naive patients with genotype 1 chronic hepatitis C: a randomized controlled trial. *J. Hepatol.* **41**, 474–481 (2004).
6. Sezaki, H. *et al.* Poor response to pegylated interferon and ribavirin in older women infected with hepatitis C virus of genotype 1b in high viral loads. *Dig. Dis. Sci.* **54**, 1317–1324 (2009).
7. Fried, M.W. Side effects of therapy of hepatitis C and their management. *Hepatology* **36**, S237–S244 (2002).
8. Pascu, M. *et al.* Sustained virological response in hepatitis C virus type 1b infected patients is predicted by the number of mutations within the NS5A-ISDR: a meta-analysis focused on geographical differences. *Gut* **53**, 1345–1351 (2004).
9. Shirakawa, H. *et al.* Pretreatment prediction of virological response to peginterferon plus ribavirin therapy in chronic hepatitis C patients using viral and host factors. *Hepatology* **48**, 1753–1760 (2008).
10. Akuta, N. *et al.* Predictive factors of early and sustained responses to peginterferon plus ribavirin combination therapy in Japanese patients infected with hepatitis C virus genotype 1b: amino acid substitutions in the core region and low-density lipoprotein cholesterol levels. *J. Hepatol.* **46**, 403–410 (2007).
11. Walsh, M.J. *et al.* Non-response to antiviral therapy is associated with obesity and increased hepatic expression of suppressor of cytokine signalling 3 (SOCS-3) in patients with chronic hepatitis C, viral genotype 1. *Gut* **55**, 529–535 (2006).
12. Gao, B., Hong, F. & Radaeva, S. Host factors and failure of interferon-alpha treatment in hepatitis C virus. *Hepatology* **39**, 880–890 (2004).
13. Matsuyama, N. *et al.* The dinucleotide microsatellite polymorphism of the IFNAR1 gene promoter correlates with responsiveness of hepatitis C patients to interferon. *Hepatol. Res.* **25**, 221–225 (2003).
14. Tsukada, H. *et al.* A polymorphism in MAPKAPK3 affects response to interferon therapy for chronic hepatitis C. *Gastroenterology* **136**, 1796–1805 (2009).
15. Nishida, N. *et al.* Evaluating the performance of Affymetrix SNP Array 6.0 platform with 400 Japanese individuals. *BMC Genomics* **9**, 431 (2008).
16. Kotenko, S.V. *et al.* IFN-λs mediate antiviral protection through a distinct class II cytokine receptor complex. *Nat. Immunol.* **4**, 69–77 (2003).
17. Sheppard, P. *et al.* IL-28, IL-29 and their class II cytokine receptor IL-28R. *Nat. Immunol.* **4**, 63–68 (2003).
18. Ank, N. *et al.* An important role for type III interferon (IFN-lambda/IL-28) in TLR-induced antiviral activity. *J. Immunol.* **180**, 2474–2485 (2008).
19. Marcello, T. *et al.* Interferons alpha and lambda inhibit hepatitis C virus replication with distinct signal transduction and gene regulation kinetics. *Gastroenterology* **131**, 1887–1898 (2006).
20. Desmet, V.J., Gerber, M., Hoofnagle, J.H., Manns, M. & Scheuer, P.J. Classification of chronic hepatitis: diagnosis, grading and staging. *Hepatology* **19**, 1513–1520 (1994).